



CARLO GAVAZZI SPACE SpA

ACOP

<i>Doc. Type:</i> REPORT		<i>DRD N°:</i> E18	
<i>Doc. N°:</i> ACP-RP-CGS-006	<i>Issue:</i> 2	<i>Date:</i> Oct. 2005	<i>Page</i> 1 <i>Of</i> 44
<i>Title :</i> THERMAL ANALYSIS AND DESIGN REPORT			

	<i>Name & Function</i>	<i>Signature</i>	<i>Date</i>	<i>DISTRIBUTION LIST</i>		
				N	A	I
<i>Prepared by:</i>	ACOP Team					
<i>Approved by:</i>	M. Grilli D. Laplena C. Cinquepalmi					
<i>Application authorized by:</i>	C. Pini					
Customer / Higher Level Contractor						
<i>Accepted by:</i>						
<i>Approved by:</i>						
				<i>N=Number of copy A=Application I=Information</i>		

<i>Data Management:</i> _____ <i>Signature</i> <i>Date</i>	<i>File:</i> ACP-RP-CGS-006_issue2.doc
---	--



CARLO GAVAZZI SPACE SpA

ACOP

THERMAL ANALYSIS AND DESIGN REPORT

Doc N°:

ACP-RP-CGS-006

Issue:

2

Date:

Oct. 2005

Page

2

of

44

CHANGE RECORD

<i>ISSUE</i>	<i>DATE</i>	<i>CHANGE AUTHORITY</i>	<i>REASON FOR CHANGE AND AFFECTED SECTIONS</i>
1	Jan. 2005	First issue	
2	Oct. 2005	CDR data package	Design maturity. All sections affected.

 CARLO GAVAZZI CARLO GAVAZZI SPACE SpA	<h1>ACOP</h1>	<i>Doc N°:</i> ACP-RP-CGS-006
	THERMAL ANALYSIS AND DESIGN REPORT	<i>Issue:</i> 2 <i>Date:</i> Oct. 2005
		<i>Page</i> 4 <i>of</i> 44

TABLE OF CONTENT

1	SCOPE OF THE DOCUMENT	5
2	DOCUMENTS.....	5
2.1	APPLICABLE DOCUMENTS	5
2.2	REFERENCE DOCUMENTS	6
3	DEFINITIONS AND ACRONYMS	6
4	SYSTEM DESCRIPTION.....	10
5	THERMAL CONTROL CONCEPT AND THERMAL DESIGN DESCRIPTION	13
5.1	HARD DISK DRIVES.....	14
5.2	ELECTRIC BOARDS.....	14
5.2.1	SBC BOARD.....	15
5.2.2	POWER SUPPLY BOARD	15
5.3	LCD MONITOR.....	16
6	THERMAL REQUIREMENTS	17
6.1	BOUNDARY TEMPERATURES AND THERMAL INTERFACES.....	19
7	THERMAL LOADS.....	20
7.1	HDD POWER DISSIPATION	20
7.2	ELECTRONIC BOARDS POWER DISSIPATION.....	21
7.3	LCD AND CONTROL BOARD POWER DISSIPATION.....	23
8	MODEL DESCRIPTION AND THERMAL ANALYSIS	24
8.1	THERMAL AND FLUIDIC MODEL DESCRIPTION	24
8.2	ANALYSIS CASES	26
9	ANALYSIS RESULTS	27
9.1	CASE 1: OUTLET FAN ON AND INLET FAN OFF.....	27
9.2	CASE 2: INLET FAN ON AND OUTLET FAN OFF.....	36
9.3	SUMMARY OF THE RESULTS IN CASE 1 AND 2	41
9.4	CASE 3: BOTH FANS FAILED.....	42
9.5	HEAT REJECTION TO THE ENVIRONMENT AND ADJACENT LOCKERS	43
10	CONCLUSIONS.....	44

 CARLO GAVAZZI CARLO GAVAZZI SPACE SpA	<h1>ACOP</h1>	<i>Doc N°:</i> ACP-RP-CGS-006
	THERMAL ANALYSIS AND DESIGN REPORT	<i>Issue:</i> 2 <i>Date:</i> Oct. 2005 <i>Page</i> 5 <i>of</i> 44

1 SCOPE OF THE DOCUMENT

This report describes ACOP thermal design for the purpose of accomplishing the internal (components) and external (Expressa Rack) temperature requirements.

The thermal control concept for the boards, the LCD and the hard disk drives (HDDs) are detailed in order to provide more solid evidences of the predicted working temperatures.

2 DOCUMENTS

2.1 APPLICABLE DOCUMENTS

AD	Doc. Number	Issue / Date	Rev.	Title / Applicability
1	SSP 52000-IDD-ERP	D / 6/08/03		EXpedite the PROcessing of Experiments to Space Station (EXPRESS) Rack Payloads Interface Definition Document
2	NSTS/ISS 13830	C / 01/12/1996		Implementation Procedures for Payloads System Safety Requirements – For Payloads Using the STS & ISS.
3	JSC 26493	17/02/1995		Guidelines for the preparation of payload flight safety data packages and hazard reports.
4	SSP 50004	April 1994		Ground Support Equipment Design requirements
5	SSP-52000-PDS	March 1999	B	Payload Data Set Blank Book
6	SSP 57066	October 28, 2003		Standard Payload Integration Agreement for EXPRESS/WORF Rack Payloads
7	GD-PL-CGS-001	3 / 17/03/99		PRODUCT ASSURANCE & RAMS PLAN
8	SSP 52000 PAH ERP	Nov. 1997		Payload Accommodation Handbook for EXPRESS Rack
9	SSP 50184	D / Feb. 1996		Physical Media, Physical Signaling & link-level Protocol Specification for ensuring Interoperability of High Rate Data Link Stations on the International Space Program
10	SSP 52050	D / 08/06/01		S/W Interface Control Document for ISPR ***ONLY FOR HRDL, SECTION 3.4 ***
11	ECSS-E-40	A / April 1999	13	Software Engineering Standard
12	AMS02-CAT-ICD-R04	29/08/2003	04	AMS02 Command and Telemetry Interface Control document. Section AMS-ACOP Interfaces
13	SSP 52000-PVP-ERP	Sept. 18, 2002	D	Generic Payload Verification Plan EXpedite the PROcessing of Experiments to Space Station (EXPRESS) Rack Payloads
14	NSTS 1700.7B	Rev. B Change Packet 8 / 22.08.00		Safety Policy and Requirements for Payloads using the STS
15	NSTS 1700.7B Addendum	Rev. B Change Packet 1 01.09.00		Safety Policy and Requirements for Payloads using the International Space Station
16	SSP 52005	Dec. 10, 1998		Payload Flight equipment requirements and guidelines for safety critical structures
17	NSTS 18798B	Change Packet 7 10.00		Interpretation of NSTS Payload Safety Requirements
18	MSFC-HDBK-527	15/11/86	E	Materials selection list for space hardware systems Materials selection list data
19	GD-PL-CGS-002	1/ 12-02-99		CADM Plan
20	GD-PL-CGS-004	2/07-04-03		SW Product Assurance Plan
21	GD-PL-CGS-005	2/09-05-03		SW CADM Plan

 CARLO GAVAZZI CARLO GAVAZZI SPACE SpA	<h1>ACOP</h1>	Doc N°: ACP-RP-CGS-006
	THERMAL ANALYSIS AND DESIGN REPORT	Issue: 2 Date: Oct. 2005 Page 6 of 44

2.2 REFERENCE DOCUMENTS

RD	Doc. Number	Issue / Date	Rev.	Title
1	GPQ-MAN-02	1		Commercial, Aviation and Military (CAM) Equipment Evaluation Guidelines for ISS Payloads Use
2	BSSC (96)2	1 / May 96		Guide to applying the ESA software engineering standards to small software projects
3	GPQ-MAN-01	2 / Dec. 98		Documentation Standard for ESA Microgravity Projects
4	MS-ESA-RQ-108	1 / 28-Sep-2000		Documentation Requirements For Small And Medium Sized MSM Projects
5	PSS-05			Software Engineering Standards
6	GPQ-010	1 / May 95	A	Product Assurance Requirements for ESA Microgravity Payload. Including CN 01.
7	GPQ-010-PSA-101	1		Safety and Material Requirements for ESA Microgravity Payloads
8	GPQ-010-PSA-102	1		Reliability and Maintainability for ESA Microgravity Facilities (ISSA). Including CN 01
9	FLOTHERM/IN/1000/1/0	2000		Introduction to FLOTHERM
10	FLOTHERM/MM/1000/1/0	2000		Guide to Defining the Mathematical Model
11	John Wiley & Sons, Inc.	1996		Fundamentals of heat and Mass Transfer
12	Transactions of the ASME, Vol.77	Nov., 1955		Numerical Solutions for Laminar-flow heat Transfer in Circular Tubes
13	Mechanical Eng. Dep., University of Kansas, Lawrence	July, 1982		Convective Heat Transfer
14	SSP 52000-IDD-ERP	E / 09/09/03		EXpedite the PROcessing of Experiments to Space Station (EXPRESS) Rack Payloads Interface Definition Document
15	ACD-Requirements-Rev-BL	September 2005	Base Line	ACOP Common Design Requirements Document

3 DEFINITIONS AND ACRONYMS

A

AAA	Avionics Air Assembly
ABCL	As-Built Configuration data List
ACOP	AMS-02 Crew Operation Post
ACOP-SW	ACOP Flight Software
ADP	Acceptance Data Package
AMS-02	Alpha Magnetic Spectrometer 02
APS	Automatic Payload Switch
AR	Acceptance Review
ASI	Agenzia Spaziale Italiana (<i>Italian Space Agency</i>)
ATP	Authorization To Proceed

B

BC	Bus Coupler
BDC	Baseline Data Collection
BDCM	Baseline Data Collection Model

C

CAD	Computer Aided Design
CCB	Configuration Control Board
CCSDS	Consultative Committee on Space Data Standards (standard format for data transmission)
C&DH	Command & Data Handling
CDR	Critical Design Review
CGS	Carlo Gavazzi Space
CI	Configuration Item



CARLO GAVAZZI SPACE SpA

ACOP

THERMAL ANALYSIS AND DESIGN REPORT

Doc N°:

ACP-RP-CGS-006

Issue:

2

Date:

Oct. 2005

Page

7

of

44

CIDL Configuration Item data List
CM Configuration Management
COTS Commercial Off The Shelf
cPCI CompactPCI (Euro Card sized standard interface to the PCI)
CSCI Computer Software Configuration Item
CSIST Chung Shan Institute of Science and Technology

D

DCL Declared Components List
DIL Deliverable Items List
DIO Digital Input / Output
DML Declared Materials List
DMPL Declared Mechanical Parts List
DPL Declared Processes List
DRB Delivery Review Board
DRD Document Requirements Description

E

EEE Electrical, Electronic & Electromechanical
EGSE Electrical Ground Support Equipment
EM Engineering Model
ER EXPRESS Rack
ERL EXPRESS Rack Laptop
ERLC EXPRESS Rack Laptop Computer
ERLS EXPRESS Rack Laptop Software
EMC Electro-Magnetic Compatibility
ESA European Space Agency
EXPRESS EXPedite the PROcessing of Experiments to Space Station

F

FEM Finite Element Model
FFMAR Final Flight Model Acceptance Review
FLASH Rewriteable persistent computer memory
FM Flight Model
FMECA Failure Modes, Effects & Criticalities Analysis
FPGA Field Programmable Gate Array
FSM Flight Spare Model

G

GIDEP Government Industry Data Exchange Program
GSE Ground Support Equipment

H

HCOR HRDL Communications Outage Recorder
HD Hard Drive
HDD Hard Disk Drive
HRDL High Rate Data Link
HRFM High Rate Frame Multiplexer
HW Hardware

I

ICD Interface Control Document
I/F Interface
IRD Interface Requirements Document
ISPR International Space-station Payload Rack
ISS International Space Station

J

JSC Johnson Space Center

K

KIP Key Inspection Point
KSC Kennedy Space Center
KU-Band High rate space to ground radio link



CARLO GAVAZZI SPACE SpA

ACOP

THERMAL ANALYSIS AND DESIGN REPORT

Doc N°:

ACP-RP-CGS-006

Issue:

2

Date:

Oct. 2005

Page

8

of

44

L

LAN Local Area Network
LCD Liquid Crystal Display
LFM Low Fidelity Model
LRDL Low Rate Data Link

M

MDL Mid-Deck Locker
MGSE Mechanical Ground Support Equipment
MIP Mandatory Inspection Point
MMI Man Machine Interface
MPLM Multi-Purpose Logistic Module
MRDL Medium Rate Data Link

N

NA Not Applicable
NASA National Aeronautics and Space Administration
NCR Non Conformance Report
NDI Non Destructive Inspection
NRB Non-conformance Review Board
NSTS National Space Transportation System (Shuttle)

O

OLED Organic Light-Emitting Diode
ORU Orbital Replacement Unit

P

PA Product Assurance
PCB Printed Circuit Board
PCI Peripheral Component Interconnect (personal computer bus)
PCS Personal Computer System
PDR Preliminary Design Review
PEHB Payload Ethernet Hub Bridge
PEHG Payload Ethernet Hub Gateway
PFMAR Preliminary Flight Model Acceptance Review
PLMDM Payload Multiplexer De-Multiplexer
PMC PCI (Peripheral Component Interconnect) Mezzanine Card
PMP Parts, Materials & Processes
PROM Programmable Read Only Memory
PS Power Supply

Q

QM Qualification Model

R

RFA Request For Approval
RFD Request For Deviation
RFW Request For Waiver
RIC Rack Interface Controller
ROD Review Of Design
ROM Read Only Memory
RX Reception

S

SATA Serial Advanced Transfer Architecture (disk interface)
S-Band Space to ground radio link
SBC Single Board Computer
SC MDM Station Control Multiplexer De-Multiplexer
ScS Suitcase Simulator
SDD Solid-state Disk Drive
SIM Similarity Assessment
SIO Serial Input Output
SOW Statement Of Work



CARLO GAVAZZI SPACE SpA

ACOP

THERMAL ANALYSIS AND DESIGN REPORT

Doc N°:

ACP-RP-CGS-006

Issue:

2

Date:

Oct. 2005

Page

9

of

44

SPF Single Point Failure
SRD Software Requirements Document
STS Space Transportation System (Shuttle)
SW Software

T

TBC To Be Confirmed
TBD To Be Defined
TBDCM Training & Baseline Data Collection Model
TBDCMAR TBDCM Acceptance Review
TBP To Be Provided
TCP/IP Transmission Control Protocol / Internet Protocol
TFT Thin Film Transistor
TM Telemetry
TRB Test Review Board
TRR Test Readiness Review
TRM Training Model
TX Transmission

U

UIP Utility Interface Panel
UMA Universal Mating Assembly
USB Universal Serial Bus

#

100bt Ethernet 100Mbit Specification
1553 Reliable serial communications bus

4 SYSTEM DESCRIPTION

ACOP thermal management exploits the Express Rack Avionics Air Assembly. Two fans are implemented to provide the necessary air circulation, one at the inlet and one at the outlet of ACOP backplate.

The characteristic of the AAA are described in AD1 and summarized below.

Flow rate	12 cfm to 18 cfm
Air temperature (for MDL)	18.3 °C to 29.4 °C

Fig. 4-1 AAA characteristic

Air flow is directed by means of a baffle at the outlet port, as shown in the picture.

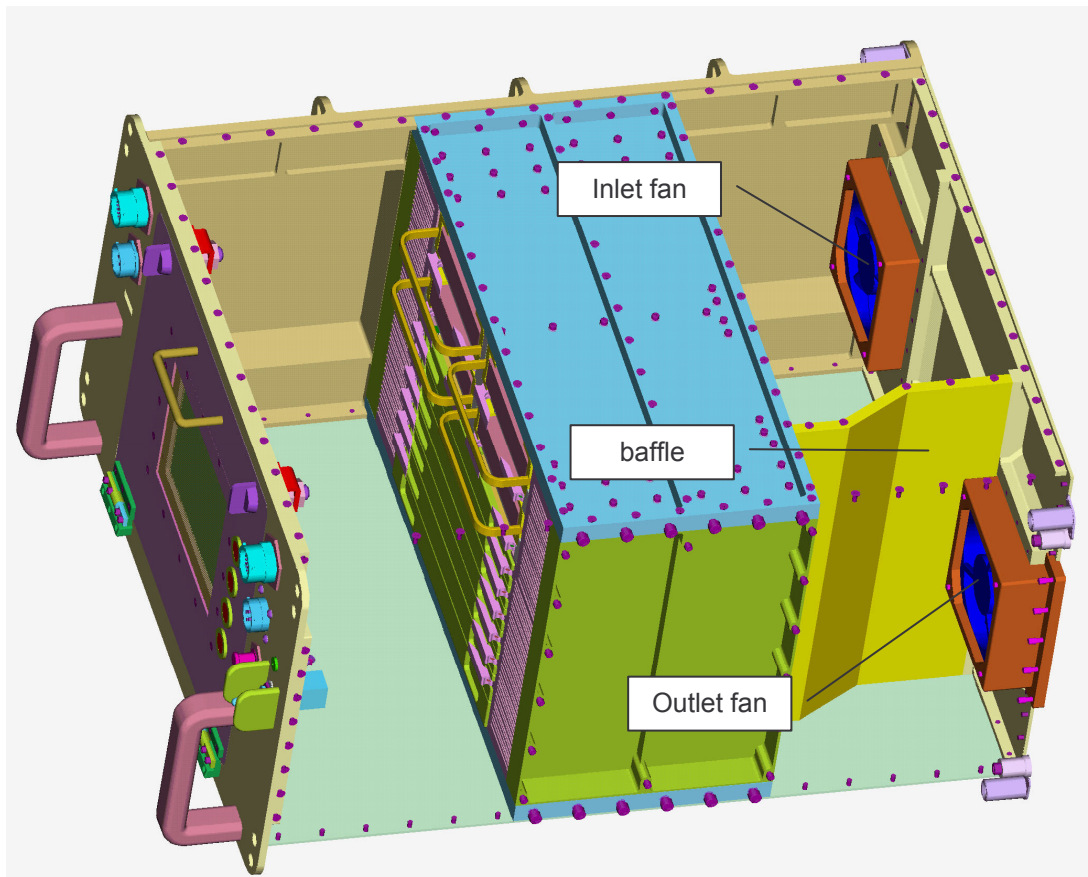


Fig. 4-2 ACOP mechanical design

The main reason to implement two fans in ACOP is redundancy. Each fan can provide enough airflow rate, the other is for redundancy.

The size of ACOP inlet and outlet ports is 110 mm by 110 mm. Both are fitted with screens, with an open area ratio of 60%, in order to filter the cooling air. The size of the fans is be 92 mm by 92 mm.

Currently the SAN ACE 92W fan of Sanyo Denki Company is selected to cool ACOP



DC Fan Motors

Splash Proof Fan □ 92mm

SAN ACE 92W

General specifications **IP55 (Dust resistant, Machine protected against water jets)**

Life expectancy 100,000 hours, indoor environment (survival rate: 90% at 60°C, rated voltage, and continuously run in a free air state)

Motor protection system .. Current cut system (with reverse-connection protection)

Dielectric strength 50/60 Hz, 500 VAC, 1 minute
(between lead conductor and frame)

Operating thermally range -10°C to +60°C (non-condensing)

Fan power lead H and F speeds, ⊕ red, ⊖ black
M and L speeds, ⊕ red, ⊖ blue

Fig. 4-3 Fan

If the fan flow rate is higher than the AAA flow rate at ACOP inlet, recirculation will occur. This will result in an inlet air temperature higher than the temperature provided by AAA. Therefore, the fans setting should be close to the minimum value 12cfm provided by EXPRESS Rack to avoid recirculation.

In the analysis the lowest AAA flow rate value has been adopted.

At each sides of the ACOP chassis, 52 alloy aluminium fins are extruded increase both of the heat transfer area and the heat transfer coefficient of the cooling air. Fins geometry is indicated in Tab. 4-1.

Number of fins at each side of the chassis	Height	Thickness	Length	Distance between two adjacent fins	Material
19 near HDD	40.3mm	1.5 mm	162 mm	2.5 mm	Al 6061
33 near boards	44.8mm				

Tab. 4-1 Geometry of ACOP Fin Channels

The effective hydraulic diameter of the fin channels is calculated to be around 4.7mm. Under this value of the effective channel diameter, the thickness of the thermal boundary layer of the fin wall can be reduced to be a small value such that for a constant Nusselt number of a laminar channel flow, the heat transfer coefficient h , is around $40 \text{ W/m}^2 \text{ } ^\circ\text{C}$.

Power dissipation is produced by every active component of each board in ACOP electronic, including the four hard disk drives. The power consumption in the form of heat conducts to the mounting board via the solder leads and the component case. The heat spreads to the board edge mainly via the copper layers implemented as the power and ground planes. Then, through the card-lock and the spacer fastening the boards to the retainers of the chassis, the heat conducts to the chassis. The fin channels extruded from the chassis absorb the heat to the surfaces. Finally the cooling air conveys away the heat via the forced convection.

The cooling air comes into the inlet, expands slightly in the back chamber of the inlet side and contracts as approaching to the fin channels and the HDDs. Then the air enters into the fin channels or into the gap, between the HDD board and the chassis housing, to take away the power dissipation. After coming out to the front chamber to cool or heat the LCD panel, the air goes through the fin channels at the outlet side, and then enters into the outlet baffle zone and finally goes out to the Rack via the outlet port.

 CARLO GAVAZZI SPACE SpA	<h1>ACOP</h1>	<i>Doc N°:</i> ACP-RP-CGS-006
	THERMAL ANALYSIS AND DESIGN REPORT	<i>Issue:</i> 2 <i>Date:</i> Oct. 2005 <i>Page</i> 12 <i>of</i> 44

Generally the Reynolds number of the fin channels is much less than the criteria value of 2300 for a turbulent duct flow. The heat transfer rate will be proportional to the inverse value of the effective diameter.

5 THERMAL CONTROL CONCEPT AND THERMAL DESIGN DESCRIPTION

In ACOP, there are three main subsystems that dissipate power :

- Hard Disk Drives
- Boards (ACOP-PS, ACOP-SBC, ACOP-T101, ACOP-T102, ACOP-T103, ACOP-T104)
- LCD monitor and control board

The following paragraphs describe in detail these subsystems, their thermal management.

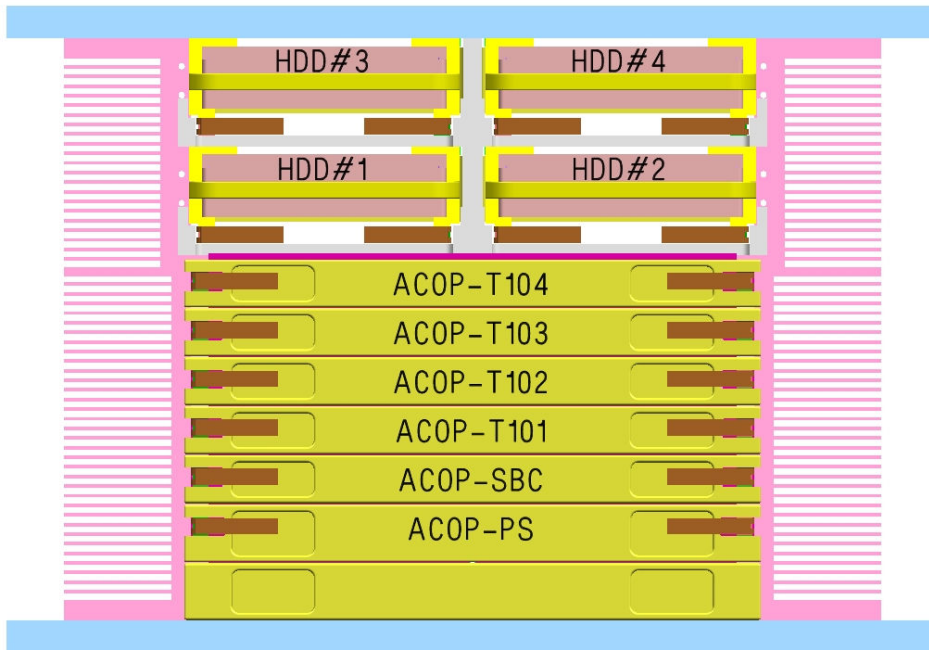


Fig. 5-1 HDD's and boards in ACOP chassis

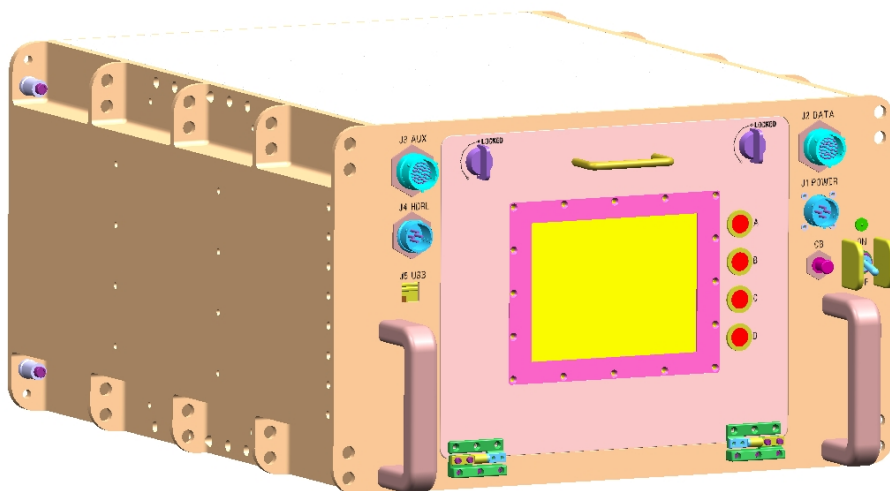


Fig. 5-2 LCD on ACOP front panel

 CARLO GAVAZZI CARLO GAVAZZI SPACE SpA	<h1>ACOP</h1>	Doc N°: ACP-RP-CGS-006
	THERMAL ANALYSIS AND DESIGN REPORT	Issue: 2 Date: Oct. 2005 Page 14 of 44

5.1 HARD DISK DRIVES

Four hard disk drives, installed in the ACOP top chassis, are used to record the data collected by AMS-02. The hard disk drives (HDD) use a heat sink to conduct the heat to the HDD edge.

The commercial hard disk drive has a control board that will dissipate a maximum power of 3.5W during operations. For commercial equipments, e.g. personal computers, the power dissipation produced by the control board will be transferred away by forced cooling air.

The gap between the HDD control board and the chassis housing can be designed to conduct the cooling air. The gap distance is designed to be around 11mm. As a result, the cooling air can cool down the components on the board and the board surface straightforward.

Between the control board and the HDD heat sink an electrical insulator is implemented to insulate the components and the heat sink electrically but conduct the power dissipation to the heat sink effectively. Thus, an assumption of an air gap of around 0.3mm is made to calculate the conductance between the board and the heat sink.

Each HDD is mounted on a caddy. The caddy is then inserted into one of the four top room of ACOP chassis. Top of the caddy is also a main thermal path for the HDD's power dissipation.

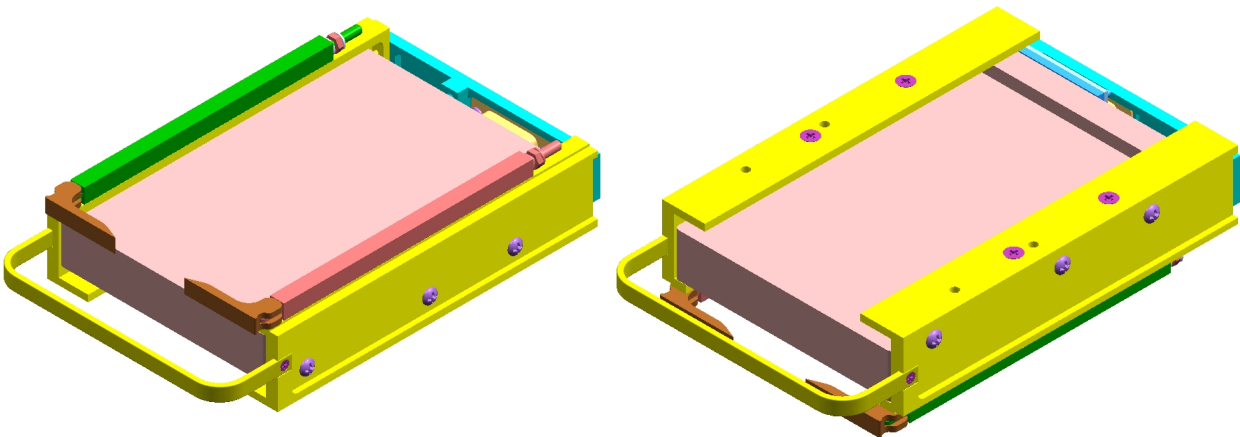


Fig. 5-3 HDD Caddy

The caddy is mounted on the chassis housing by two card-locks with the caddy top flanges contacting on the housing. Since thermal filler is not used at the interface, the interface contact conductance between the caddy and the chassis is assumed to be $0.1 \text{ W/cm}^2\text{°C}$.

For the interface between the HDD heat sink and the Caddy, the contact conductance is assumed to be $0.05 \text{ W/cm}^2\text{°C}$.

The power dissipation of the HDD drive is conducted by the heat sink to the HDD edge. Thus the thermal load from the drive can be effectively conducted to the ACOP chassis via the Caddy.

5.2 ELECTRIC BOARDS

The power dissipation of components on the described boards is mainly conducted through the copper layers of power planes and of ground planes to the board edge and then via the spacers, which are fixed to the chassis by card-locks, to the chassis and spreads to the fins, and finally transfers to the cooling air.

 CARLO GAVAZZI CARLO GAVAZZI SPACE SpA	<h1>ACOP</h1>	<i>Doc N°:</i> ACP-RP-CGS-006
	THERMAL ANALYSIS AND DESIGN REPORT	<i>Issue:</i> 2 <i>Date:</i> Oct. 2005 <i>Page</i> 15 <i>of</i> 44

Also a slot for spare board is foreseen by the system design, and a spare board has been considered also in the analysis (ACOP-T104).

The effective thickness of the copper layers will be the main factor to determine the component working temperature on the PCBs, since thermal conductivity of the PCBs material polyimide 0.19 W/m K, while the thermal conductivity of the copper layers 398W/mK.

Board surface emissivity is assumed 0.5 .

For ground and power planes of the PCBs, the weight is etched out by around 10%, and about 90% of the copper weight is utilized to conduct the thermal load of components to the PCB edge.
 For signal planes, nearly all the layer is etched away. Here, we assume around 5% of the weight left for conduction.

The SBC and the PS board have components with larger power dissipation than assumed in PDR (microprocessor EMPPC750L and a regulator on SBC and DC-DC converters on PS). For these components, heat sinks are designed-in to enhance the thermal conductance, leading to a decrease of the component working temperature.

5.2.1 SBC BOARD

For the SBC board, an effective thickness of 0.3885mm for the copper layers can lead to the board centre with an increase temperature around 25°C to the board edge.

The value of the thermal resistance between the microprocessor EMPPC750L Die and the board depends on the type of the mounted board and varies from 3.8 to 7.6 °C/W (according to the data sheet). A mean value to be around 5 °C/W in the thermal model.

A heat sink of alloy aluminium is designed to mount on the microprocessor top surface and fasten by using screws. The heat sink is extended to the board edge and contacts with a spacer to conduct the thermal load effectively.

Between the microprocessor and the heat sink, the thermal filler T642 is used to fill the gap of the interface. The filler T642 only provides a thermal resistance around 2 °C/W in a similar application. Here we will use the thermal filler with a much higher thermal conductivity 17 W/m K than that of T642, named Sarcon XR-m produced by Fujipoly Ltd. Although the interface thermal conductance will be enhanced to be far more than 0.5W/°C, under conservative calculations, the thermal resistance of filling the filler T642 is taken here in the thermal model of ACOP to calculate the microprocessor temperature.

In addition to the microprocessor, the regulator with a small size also dissipates a power rate around 2.0 W. If the regulator is not managed properly to conduct the thermal load to the chassis, the working temperature will far beyond other components. Thus, the regulator is put at the edge of the board and is mounted on a copper layer to be the heat sink.

5.2.2 POWER SUPPLY BOARD

The main components of this board are three DC-DC converters. For the worst condition, the board will dissipate around 23.4W. An aluminium alloy plate with a thickness of 3mm is adopted to be the heat sink by mounting the DC-DC converters on the heat sink top surface. To improve the thermal contact between the DC-DC converters and the heat sink the thermal filler Fujipoly Sarcon XR-m is adopted (conductivity 17W/m°C and thickness of 0.3mm).

 CARLO GAVAZZI CARLO GAVAZZI SPACE SpA	<h1>ACOP</h1>	Doc N°: ACP-RP-CGS-006
	THERMAL ANALYSIS AND DESIGN REPORT	Issue: 2 Date: Oct. 2005 Page 16 of 44

In the thermal model the thermal filler conductance has been assumed $2.0 \text{ W/cm}^2\text{°C}$ (interface conductance between the heat sink and the converter 6193E-S3.3F); a conservative value..
 The thermal contact conductance of the interface between the heat sink and the chassis is also adopted as $0.1 \text{ W/cm}^2\text{K}$ as previous assumptions for a conservative consideration because only by applying the card-lock to fasten the heat sink on the chassis retainers without any thermal filler.

5.3 LCD MONITOR

LCD thermal details are not indicated by the manufacturer. The model assumes the LCD as a 1 mm thick Al plate, with power applied as indicated in section 7.3. LCD is protected by a Lexan panel having thermal conductivity 0.2 W/m K .

The contact surface area of the Lexan panel to the front panel is assumed to be its thickness by the height and neglecting the contact resistance.

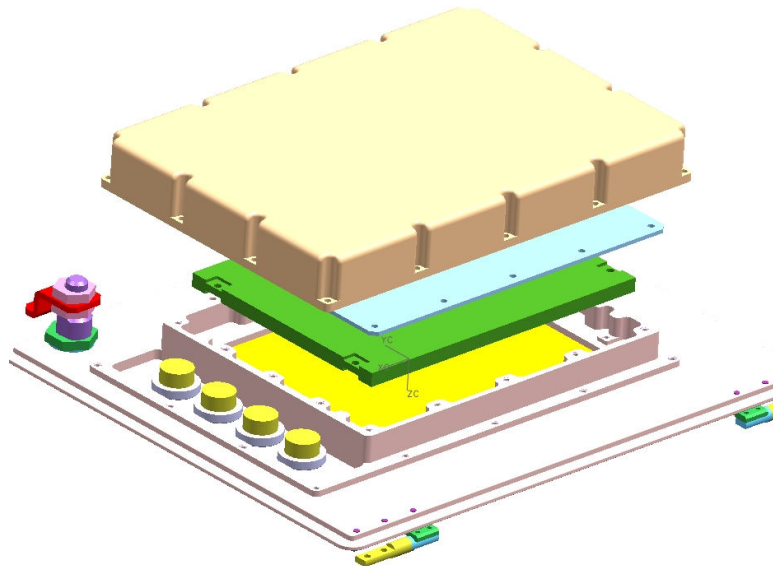


Fig. 5-4 LCD mounting details (yellow=Lexan transparent shield, green=LCD monitor, blue=control board)

6 THERMAL REQUIREMENTS

The internal temperature requirements are summarized in Tab. 6-1.

Description	Temperature Requirements (°C)
ACOP-SBC	85
ACOP-T101 (HRDL Interface)	70
ACOP-T102	85
ACOP-T103	85
ACOP-PS	85
LCD Monitor	60
LED	85
HDD	70

Tab. 6-1 ACOP internal temperature requirements

Tab. 6-2 shows the external temperature requirements derived from the EXPRESS Rack interface (AD1-RD6)

Description	Temperature Requirements (°C)
Average front panel surface	37
Maximum temperature on front panel surface	49
Air exhaust temperature	49

Tab. 6-2 EXPRESS Rack temperature requirements from AD1

Tab. 6-3 lists the allowable working temperature of SBC main components and PD DC-DC converters.

For the passive components, the allowable temperature is set for the component case, normally 125 or 150°C. For the main components, the microprocessor, the junction temperature is taken as the criteria to be 105 °C, and the regulator is taken the ambient temperature 80°C . For the PS board, the DC-DC converters are chosen to have the allowable temperature of 125°C at the mounting case.



CARLO GAVAZZI SPACE SpA

ACOP

THERMAL ANALYSIS AND DESIGN REPORT

Doc N°:

ACP-RP-CGS-006

Issue:

2

Date:

Oct. 2005

Page

18

of

44

Board	Component	Operating Temperature	
		min.	max.
ACOP - SBC	PQ7DV10	-20	80(Ta)
ACOP - SBC	LP2989IM2.5	-40	125(Tj)
ACOP - SBC	IBM25EMPPC750L-GBF400A2	-40	105(Tj)
ACOP - SBC	IBM25CPC700BB3B66	-40	105(Tj)
ACOP - SBC	Z9972AI	-40	85(Ta)
ACOP - SBC	A54SX32A-3PQ208I	-40	85(Ta)
ACOP - SBC	5962-9668601QXA	-55	125
ACOP - SBC	AM29LV040B-90JI	-40	85(Ta)
ACOP - SBC	AM29LV641DH90REI	-40	85(Ta)
ACOP - SBC	5962H0151701QXA	-55	125
ACOP - SBC	CXO3M-10N-SM3-33MHz	-55	125
ACOP - SBC	K4S560832C	0	85(Ta)
ACOP - SBC	MAX869LEEE	-40	85(Ta)
ACOP - SBC	MAX706SESA	-40	85(Ta)
ACOP - SBC	M83513/04-A09N	-55	200
ACOP - PS	5193E-S3.3F		125(Tc)
ACOP - PS	5680E-S05F		125(Tc)
ACOP - PS	5031E-S12		125(Tc)

Tab. 6-3 Temperature requirements of main components on SBC and PS board

 CARLO GAVAZZI CARLO GAVAZZI SPACE SpA	<h1>ACOP</h1>	<i>Doc N°:</i> ACP-RP-CGS-006
	THERMAL ANALYSIS AND DESIGN REPORT	<i>Issue:</i> 2 <i>Date:</i> Oct. 2005 <i>Page</i> 19 <i>of</i> 44

6.1 BOUNDARY TEMPERATURES AND THERMAL INTERFACES

The cooling air temperature supplied by the AAA will be in the range from 18.3 to 29.4°C, indicated in 5.3.1.3.2 of the AD1. AAA temperature is assumed 30°C for conservative analysis.

The back-plate, top-plate, two side-plates, and bottom-plate of ACOP are assumed to insulate from the outside environment according to the requirements in 5.3.1.3.7 of the applicable reference [1], “ All, Payloads shall not design to account for conducting payload heat to the rack structure”. See also section **Errore. L'origine riferimento non è stata trovata.**

The tip plate to enclose the fin channels, in order to confine and to conduct the cooling passing through the extruded fins, is also considered to insulate from the outside surrounding air, which exists between the ACOP locker and the ACOP electronic modules.

Only the front panel, seeing the inner space of the ISS cabin, has a natural convection with the cabin by a heat transfer coefficient of 0.965 W/m²°C, referred to 5.3.1.1.3 of AD1. This value is utilized in the prediction model. The ISS cabin air temperature is assumed to be 30°C, the same as the cooling air provided by AAA.

The radiation effect of the front panel including the Lexan panel to the ISS inside ambient by assuming the total exchange emissivity as 0.82.

The boundary conditions of ACOP for thermal analysis are listed in *Tab. 6-4*.

Inlet air pressure	Inlet air temperature	Value of h of front panel to ISS cabin
10.2psia	30°C	0.965 W/m ² °C

Tab. 6-4 Boundary Conditions of ACOP

7 THERMAL LOADS

Tab. 7-1 shows the power considered in ACOP thermal model assuming:

- only one fan is working at a time
- 2 HDD are working at a time and the other two are in standby mode (see issue 1)
- even if the spare board slot is not currently used in the design, thermal analysis foresees a PCB with uniform power distribution as indicated in the next table, in order to provide a worst case configuration.

Description	Power(W)
ACOP-SBC	9,90
ACOP-PS	23,39
ACOP-T103	1,65
ACOP-T102	5,02
ACOP-T101	1,65
ACOP-T104 (Spare)	4,95
DC Fan	1,68
LCD Monitor	0,80
LCD LED Backlight	4,80
LCD Video Interface board	0,10
HDD LOC 1 (standby)	1,48
HDD LOC 2 (standby)	1,48
HDD LOC 3	12,50
HDD LOC 4	12,50
Total	81,9

Tab. 7-1 ACOP Power Budget

7.1 HDD POWER DISSIPATION

According to ACOP PDR thermal analysis, the worst condition is that the working HDD's are mounted on the top of ACOP chassis. Thus, in the thermal model for CDR, the two working HDD's are implemented in the top of ACOP.

The power dissipation of the HDD's is separately allocated into the drive and the control board. The working drive dissipates the maximum power dissipation around 9W. The control board consumes around 3.5W and the thermal load is also uniformly allocated on the board in the model.

The stand-by HDD's dissipate around 1.48W each one, which is modelled at the two bottom HDD's boards uniformly.

7.2 ELECTRONIC BOARDS POWER DISSIPATION

The PS board dissipates 23.39W, contributed from the three DC-DC converters for the supplied voltages 3.3V, 5V, and 12V respectively. The components have been accommodated at the mounting site of the heat sink close to the inlet fin channels.

The power distribution on the ACOP-PS board thermal model is indicated in Fig. 7-1.

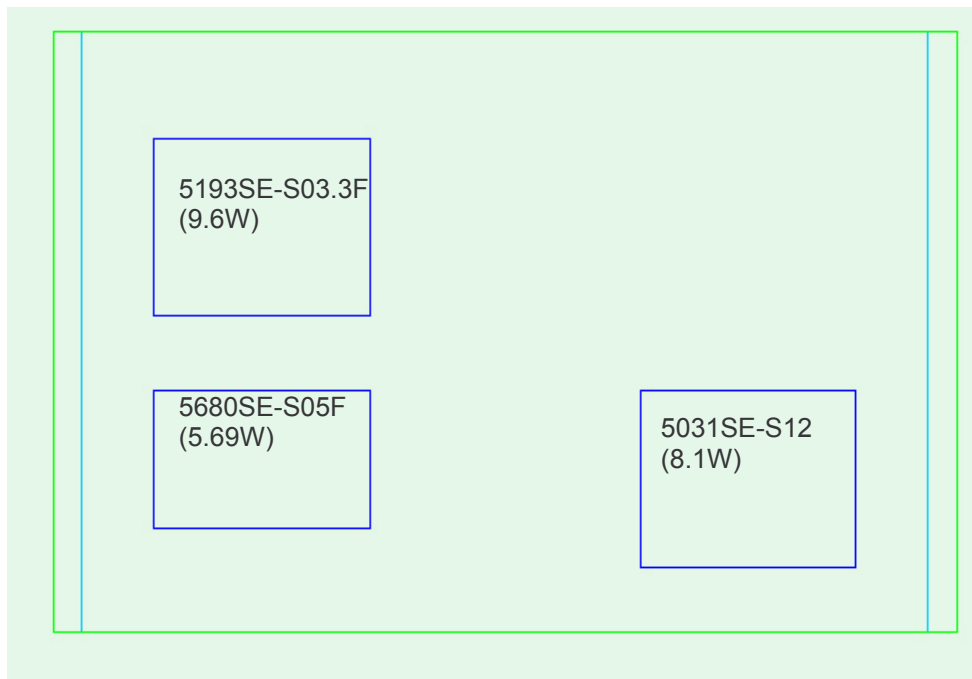


Fig. 7-1 Power distribution in the ACOP-PS board thermal model

For the SBC board, the estimated power dissipation of every component is allocated at the mounted site of the boards at component side except for the microprocessor as indicated in Tab. 7-2 SBC dissipati. The power dissipation of the microprocessor is allocated at the Die.

Fig. 7-2 gives an idea on how power is distributed throughout the board (some minor dissipating components are not indicated in the image).

<u>SBC components</u>	<u>Power in the model (mW)</u>
PQ7DV10	2000
LP2989IM2.5	70
IBM25EMPPC750L-GBF400A2	4600
IBM25CPC700BB3B66	560.7
AM29LV641DH90REI x 4	20.75 x 4
CXO3M-10N-SM3-33MHz (50ppm/50ppm/50ppm/M)	8
MAX869LEEE	0.03
MAX706SESA	1.7
K4S560832C-TC75 x 9	161.89 x 9
RT54SX32S	231
UT28F256LV x 8	57.75 x 8
MPC972FA	300
SNJ54LVTH16245AWD x 5	28.8 x 5

Tab. 7-2 SBC dissipating components

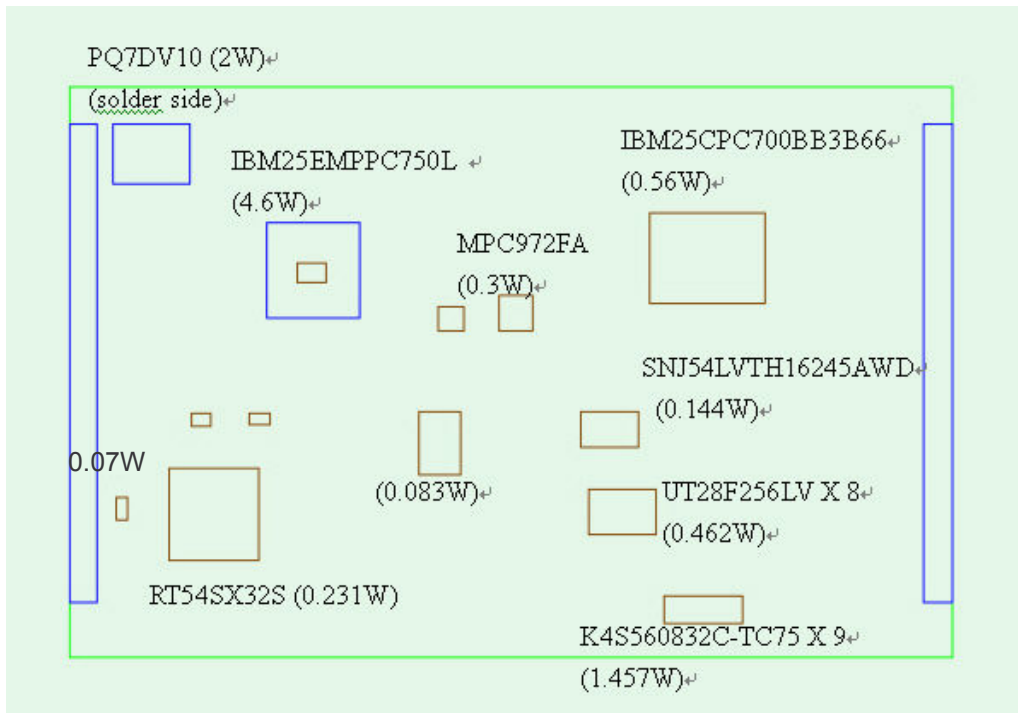


Fig. 7-2 Power distribution in the ACOP- SBC board thermal model

The ACOP- T101 board power dissipations for the main components are allocated at the mounting sites to simulate the actual condition. The power distribution on the ACOP- T101 board thermal model is indicated in Fig. 7-3.



Fig. 7-3 Power distribution in the ACOP- T101 board thermal model

For the remaining boards including SATA and Fan Control, Spare board, and the HRDL board, thermal loads are allocated uniformly on the component side of the boards in the thermal model.

7.3 LCD AND CONTROL BOARD POWER DISSIPATION

The power dissipation on the LCD monitor and control board is distributed as in Fig. 7-4.

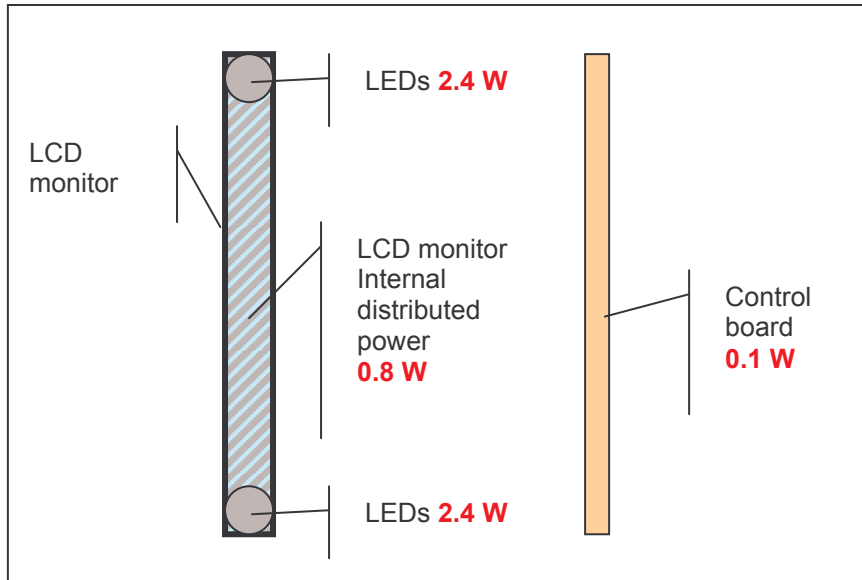


Fig. 7-4 LCD power distribution

8 MODEL DESCRIPTION AND THERMAL ANALYSIS

8.1 THERMAL AND FLUIDIC MODEL DESCRIPTION

“Flotherm” code is applied to solve the computation task, including the detailed model of the PCBs with a coupling of heat transfer and flow dynamics. The solid and the fluid domain are meshed before the calculation by employing a finite difference method.

The analyzed domain is meshed into around 0.9 million elements by using the mapped method. See Fig. 8-1.

The cross section of a fin channel gap for the cooling air passing through is divided into ten elements. Along the direction of the chassis root to the fin tip, the channel air is divided into 4 elements near the HDDs and 5 elements near the boards respectively

Along the flow direction, each fin channel is divided in 22 sections. The size of the section is not uniform and dependent on the board meshing.

It means that the element size in the fin channels is 0.25 mm for the adjacent fins.

The height of the element is much less than the other two dimensions of width and length based on the consideration of a rapid variation of the flow velocity at the cross section of the channels. Along the flow direction and the fin tip direction, the flow properties vary slightly. Thus, the element dimension along the two directions can be larger than the gap direction without a loss of accuracy.

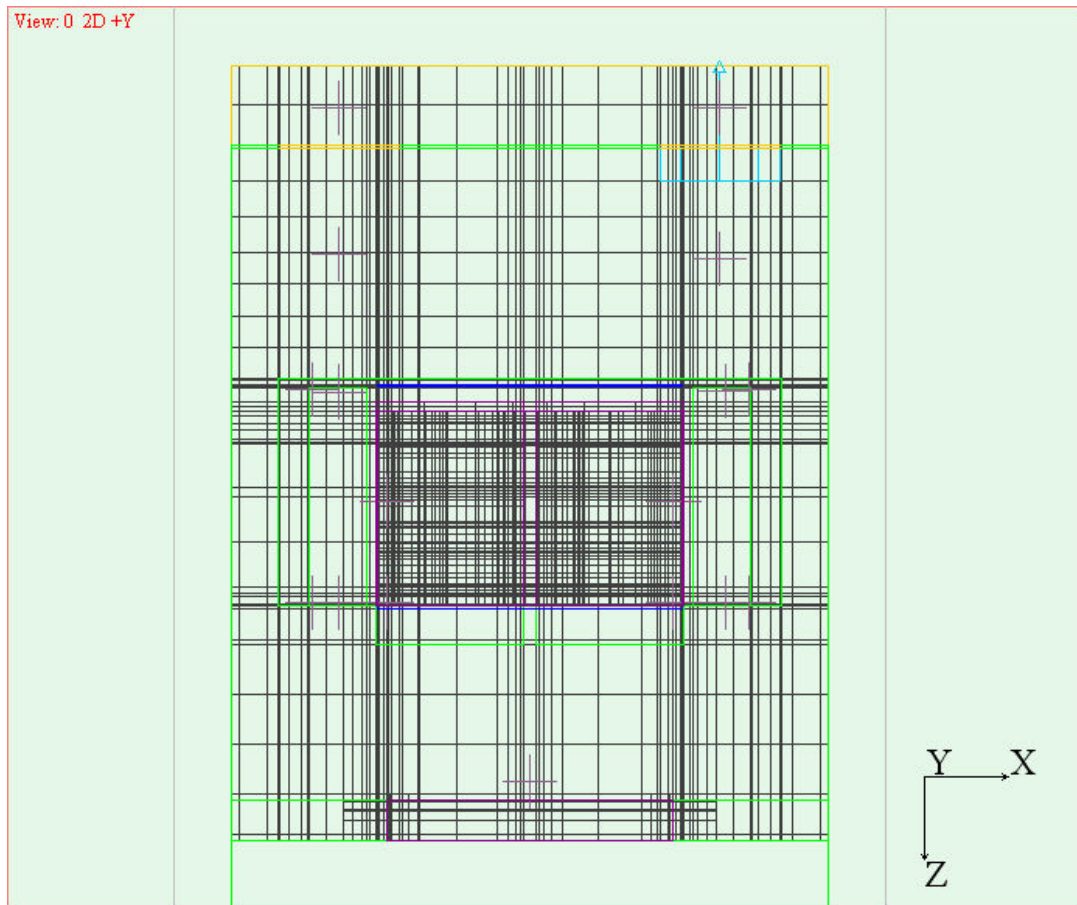


Fig. 8-1 Top view of ACOP meshed elements in the modelling

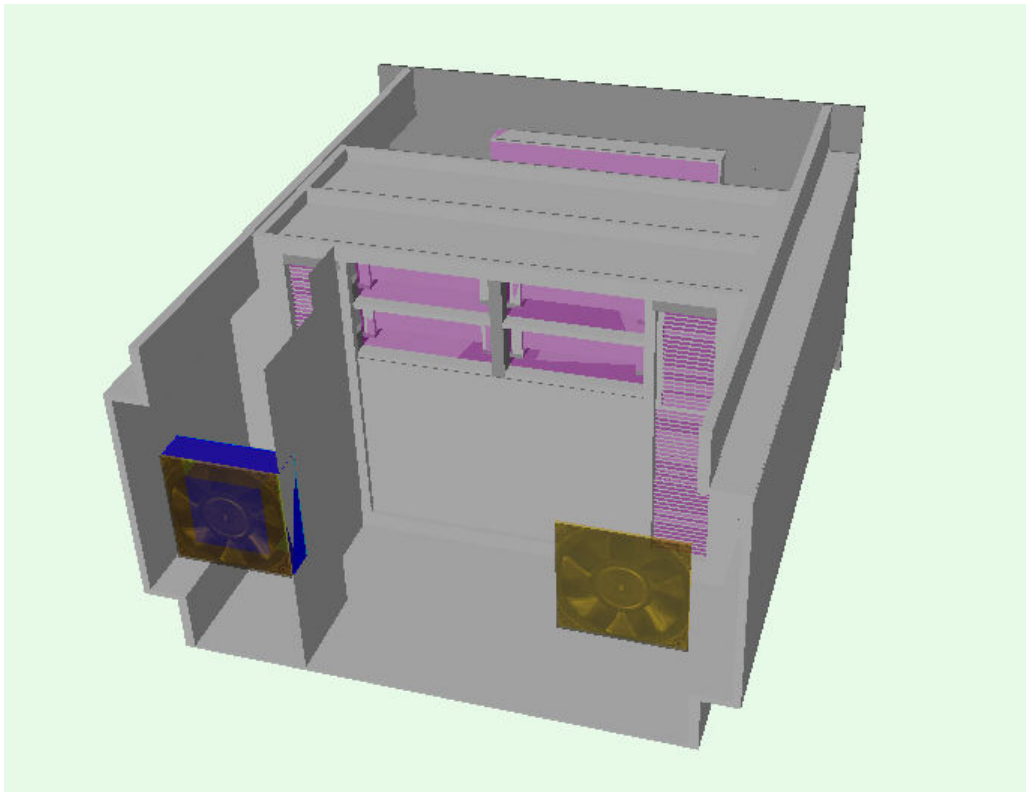


Fig. 8-2 Thermal modelling configuration of ACOP (back plate not shown)

Based on the electrical analogy, thermal model of the solid domain is established to construct a resistance-capacitance thermal network. A hybrid approach is developed in the code by utilizing the element based finite difference method to simulate conduction, and surface convection.

The thermal code is coupled with the element based finite volume method flow solver, which models air flow, fluid conduction, and convection.

Reynolds number of the outlet fin channel flow is calculated to be the order of 300 for Case 1 to show most regions of the channels belonging to a laminar flow.

The inlet and the outlet of the channels give the characteristic of turbulence flow due to the flow entry effect.

In the laminar flow regions, the turbulence effect will decay to close to null.

Thus, most of the flow regions demonstrate the characteristics of a laminar zone.

Since nearly all the thermal load of the boards and HDD's is dissipated to the cooling air via the fin channels, and most regions of the fin channels belong to the laminar flow, the computation model here adopts the laminar flow model to compute the flow properties of the analyzed domain, neglecting the turbulence effect in the entry regions with a more conserved consideration of heat transfer between the cooling air and ACOP.

The thermal conductivity of alloy aluminium 7075-T7351 is adopted as a constant value 151 W/m°C

Both the thermal and momentum wall functions utilized to calculate the heat transfer coefficient for the solid surface and the cooling air, described in the reference document [10].

 CARLO GAVAZZI CARLO GAVAZZI SPACE SpA	<h1>ACOP</h1>	Doc N°: ACP-RP-CGS-006
	THERMAL ANALYSIS AND DESIGN REPORT	Issue: 2 Date: Oct. 2005 Page 26 of 44

$$h_w = St \times \rho \times u \times C_p, \quad St = \frac{1}{Re Pr}, \quad Q_w'' = \frac{k}{y}(T - T_w) = h_w(T - T_w)$$

(1)

Where h_w is the heat transfer coefficient, St is Stanton number, ρ is the density of air at the local distance y from wall, u is the local air velocity, C_p is the air specific heat, Re is the local Reynolds number, and Pr is Prandtl number, Q_w'' is the heat flux at wall, k is a local thermal conductivity.

As the velocity, temperature and pressure fields in the airflow are calculated out, the flow properties and Reynolds number and the given Prandtl number can be applied to compute the value of h_w . Once the value of h_w at the solid surface flow passes through is obtained, the wall temperature can be calculated via Equation (1).

8.2 ANALYSIS CASES

Each fan can work independently from the other, and therefore both cases have been studied. A third case has been analysed under the assumption that both fans are failed to see the rising of ACOP temperature in this non-nominal situation.

	Number of Active Fans	Location of Fan	Flow Type of Air
Case 1	1	Outlet	Exhausting
Case 2	1	Inlet	Blowing
Case 3	0	-	No air flow

Tab. 8-1 Analysis cases

The complementary case (i.e. both fans working at 12 cfm each) has not been considered. In this case in fact, the internal flow rate will be higher than the AAA flow rate. ACOP would suck hot air from the rack environment and also internal recirculation may occur.

AD1 provides no information on how to take into account the air suction from other sources than AAA, and suggests to avoid recirculation setting the fans flow rate at the nominal value of 15 cfm (or lower).

9 ANALYSIS RESULTS

9.1 CASE 1: OUTLET FAN ON AND INLET FAN OFF

The cooling air velocity field at the central section of the fin channels for Case 1 is shown in Fig. 9-1.

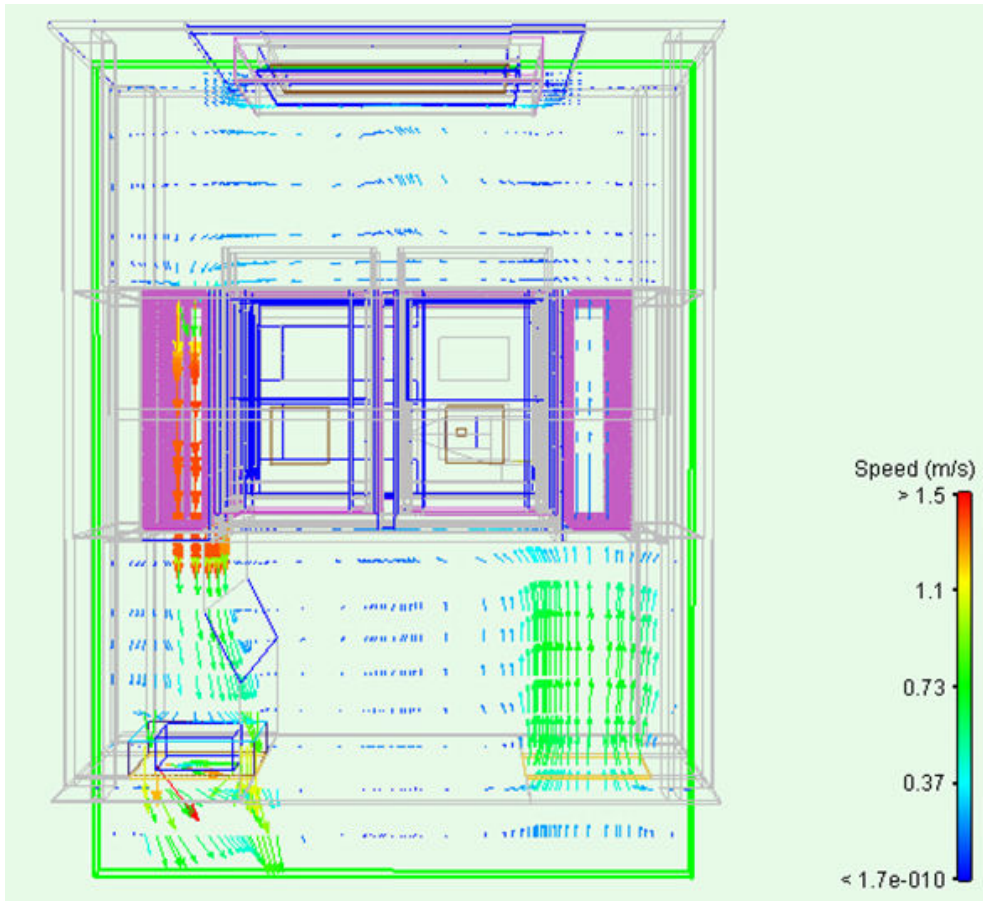


Fig. 9-1 The predicted velocity field of the cooling air in ACOP along the central section for Case 1

Since the cooling air is exhausted out from ACOP by the outlet fan, the cooling air enters ACOP back chamber via the inlet with a larger speed rate due to the inlet small area. Although entering into the back chamber with a much larger room or crossing area than the other regions, the air still moves with a slight decrease in the velocity till ahead of the HDDs and of the inlet fin channels where the flow start to separate into two parts, a large portion of the cooling air going through the HDDs gap, and the rest entering into the inlet channels. Therefore, part of the HDDs power consumption can be dissipated directly to the cooling air by forced convection and a significant decrease of the pressure loss in the fin channels is resulted from the decrease of the channel velocity.

The outlet fin channels rather than the HDDs gap are the only paths for the cooling air to go through, therefore the air velocity in the outlet fin channels is significantly larger than that in the inlet channels. Thus, the system pressure loss is mainly contributed to the friction loss in the outlet fin channels.

The predicted max. velocity is 1.5 m/sec and the mean velocity 1.0 m/sec at the outlet fin channel.

The entrance effect of in the inlet fin channels on the velocity variation is also predicted in the model. The contraction as entering into the HDD gap and the inlet fin channels can be seen. The velocity of the airflow varies smoothly in the inlet fin channel. However, since the air velocity in the inlet fin channels is small compared to the main flow velocity, at the outlet of the inlet fin channels does not produce strongly turbulent eddies due to an expansion. However, at the inlet of the outlet side fin channels, the air velocity increases. This will induce a significant pressure loss at the inlet. Similarly, the air velocity in the outlet fin channels along the cross section is quite uniform that should be in the actual confined flow. Theoretically both the flow velocity and the Reynolds number are low enough to produce a laminar flow in the fluid domain. However, at the interfaces of the fin channels and the chambers, the eddy will yield a turbulence effect to enhance the heat transfer rate. Simultaneously the pressure loss due to the turbulent eddies also happens in this region. The pressure loss will be much higher than the wall friction loss under the laminar flow. At both ends of the front panel chamber, flow impingement phenomena occur to results into the enhancement of heat transfer and of the pressure loss.

The pressure distribution of the central section for Case 1 is shown in Fig. 9-2.

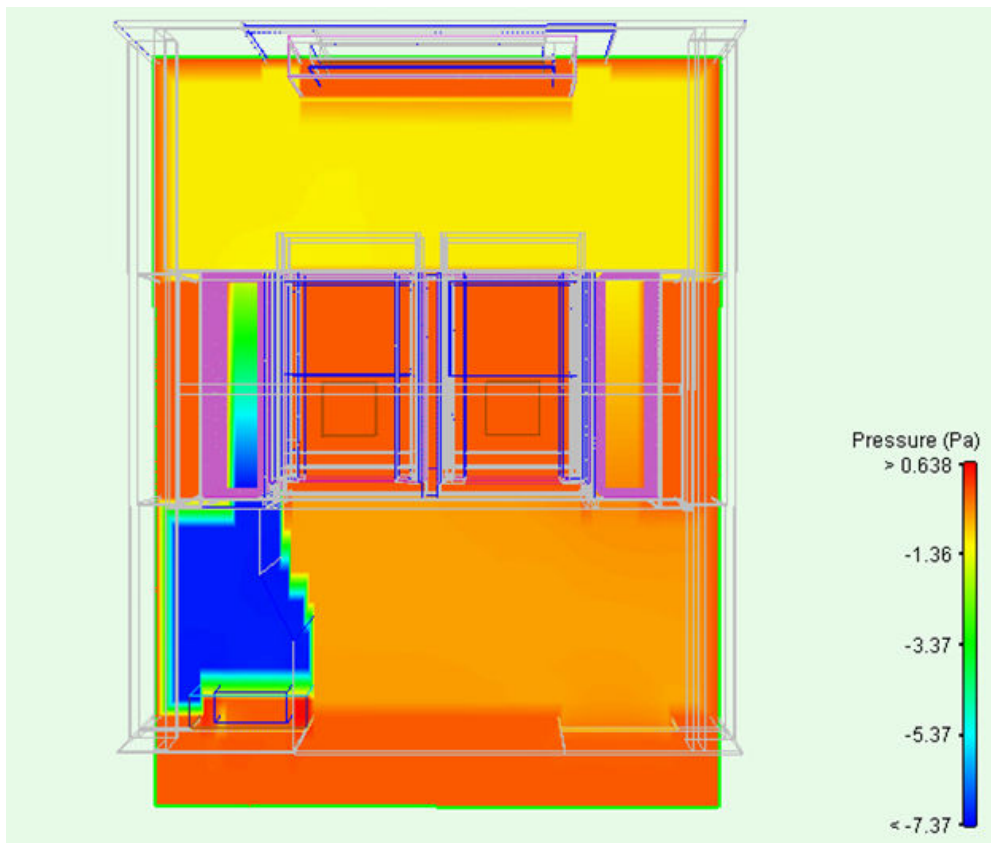


Fig. 9-2 Predicted pressure distribution of ACOP for Case 1 with outlet fan working fans

For the outlet fan working, the pressure head is largest at ACOP inlet to be around -1Pa where the negative value is due to the exhausting flow and the value of near -1Pa loss is resulted from the off inlet fan impedance and the filter pressure loss. The pressure loss in the back chamber of the inlet side is insignificant due to both of a very low friction coefficient and a low air velocity in this chamber as compared to the total loss. Since the air velocity in the inlet fin channels is as small as around 0.2 m/sec, the pressure loss in the channels is predicted around 0.5Pa, which is much lower than the total pressure head provided by the outlet fan. In the front chamber, the pressure distribution is quite uniform, resulted from the model assumption of a laminar flow. Thus, the flow eddy and impingement effect cannot be predicted in the flow model. As mentioned, while the air entering into the outlet fin channels, the velocity increases significantly,

resulting into the significant pressure loss and then the pressure loss happens in the outlet fin channels apparently due to a larger air velocity than in the inlet fin channels. Thus, as entering into the outlet side of the back chamber, the pressure nearly reaches to the minimum value around -7Pa . The pressure loss in the outlet side chamber is insignificantly due to a low friction coefficient. In summary, the pressure loss is mainly contributed from the outlet fin channels and partly from the inlet fan and filter and a small proportion from the inlet fin channels or the HDD's gap.

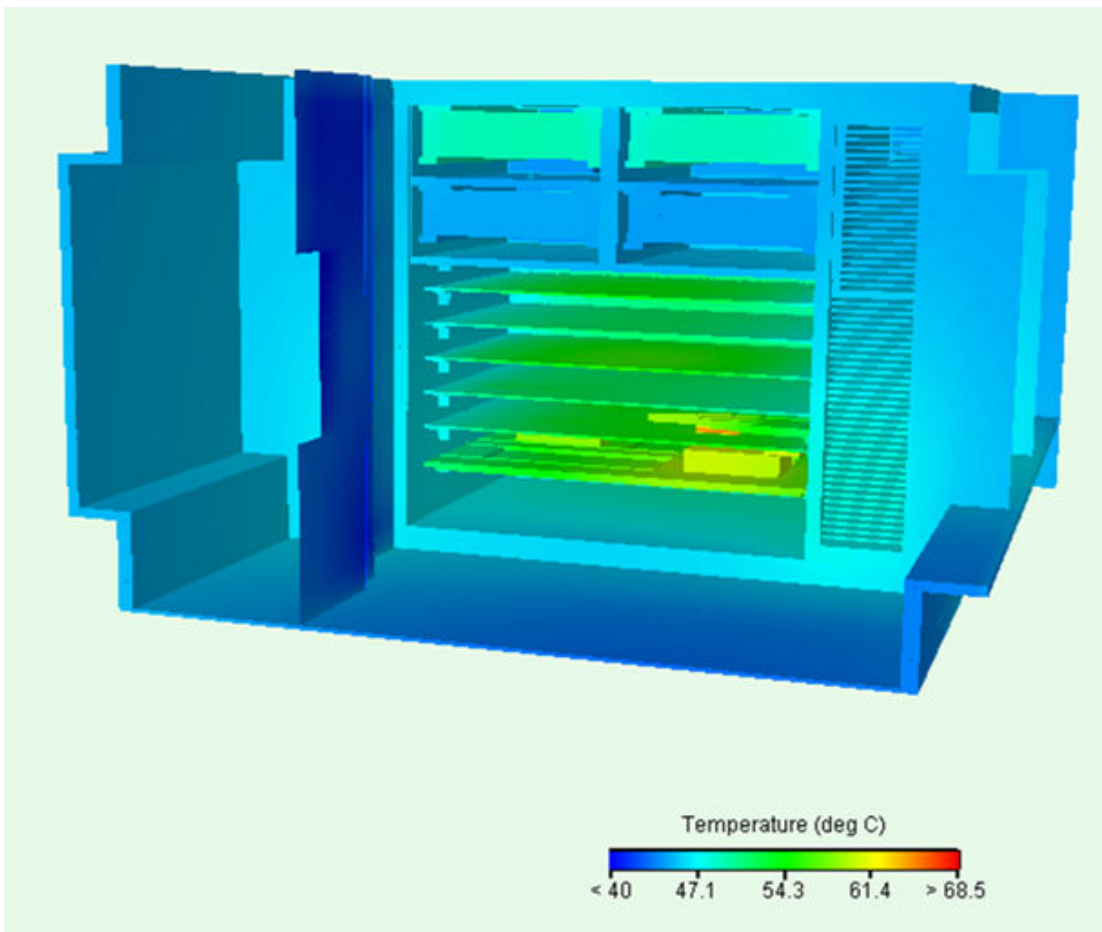


Fig. 9-3 Predicted temperature profile of ACOP for Case 1



CARLO GAVAZZI SPACE SpA

ACOP

THERMAL ANALYSIS AND DESIGN REPORT

Doc N°:

ACP-RP-CGS-006

Issue:

2

Date:

Oct. 2005

Page

30

of

44

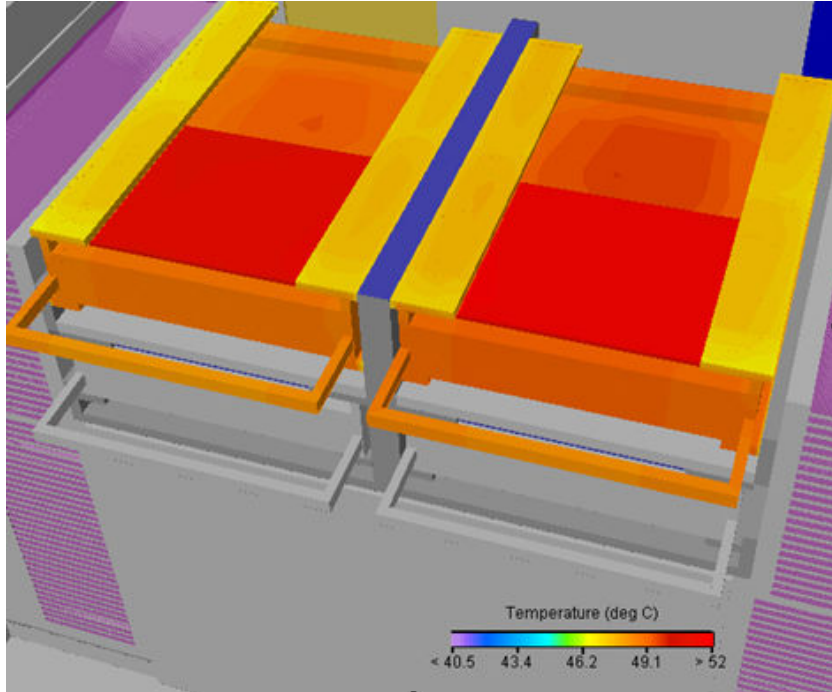


Fig. 9-4 Predicted temperature of working HDD's for Case 1.

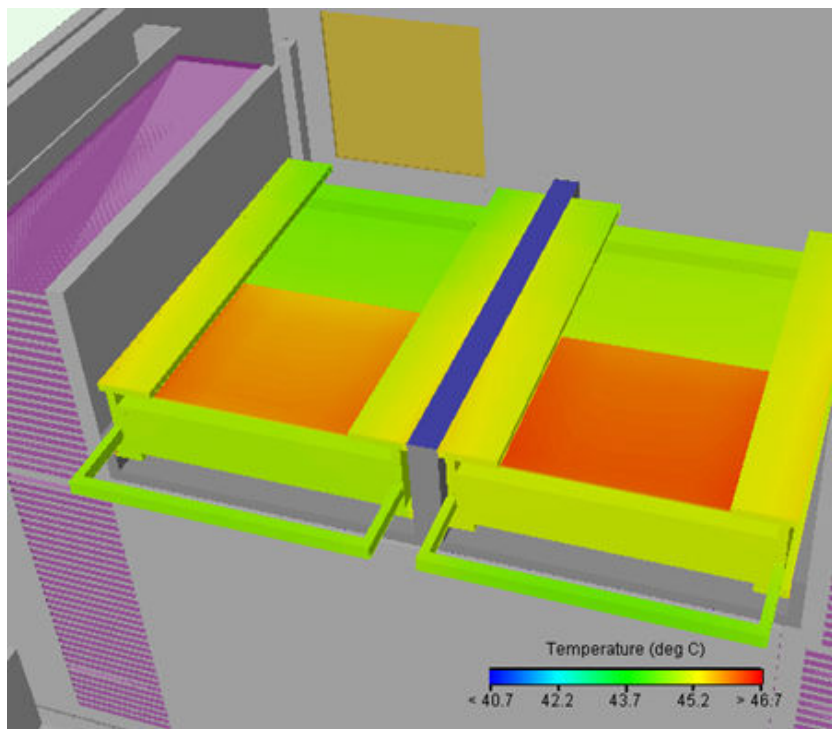


Fig. 9-5 Predicted temperature of stand by HDD's for Case 1.

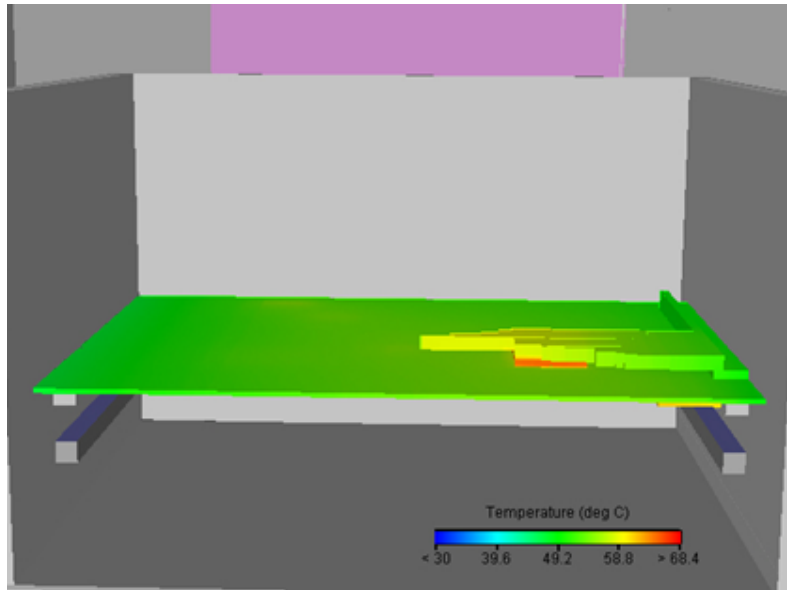


Fig. 9-6 Predicted SBC board temperature at the component side for Case 1

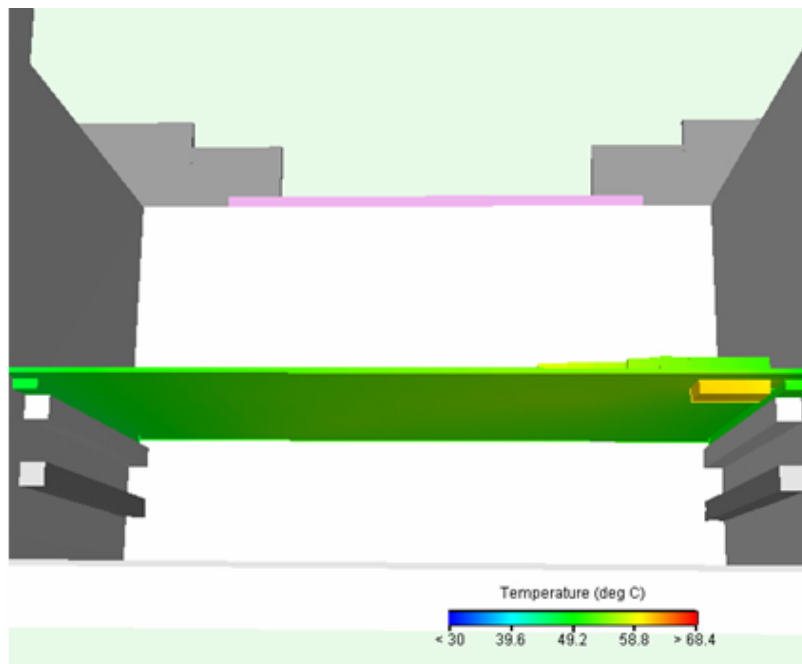


Fig. 9-7 Predicted SBC board temperature at the solder side for Case 1

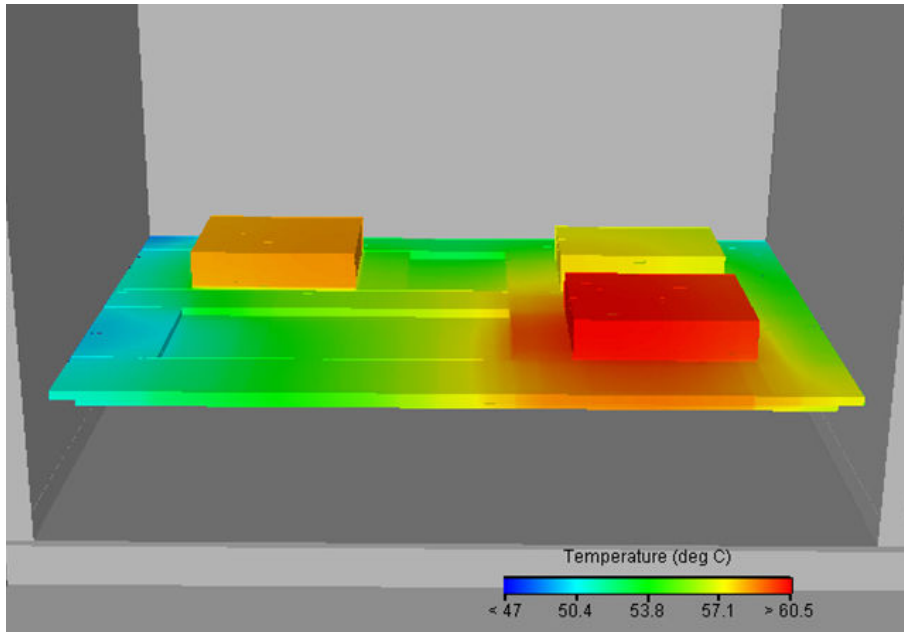


Fig. 9-8 Predicted temperature profile of Power Distribution Board for case 1

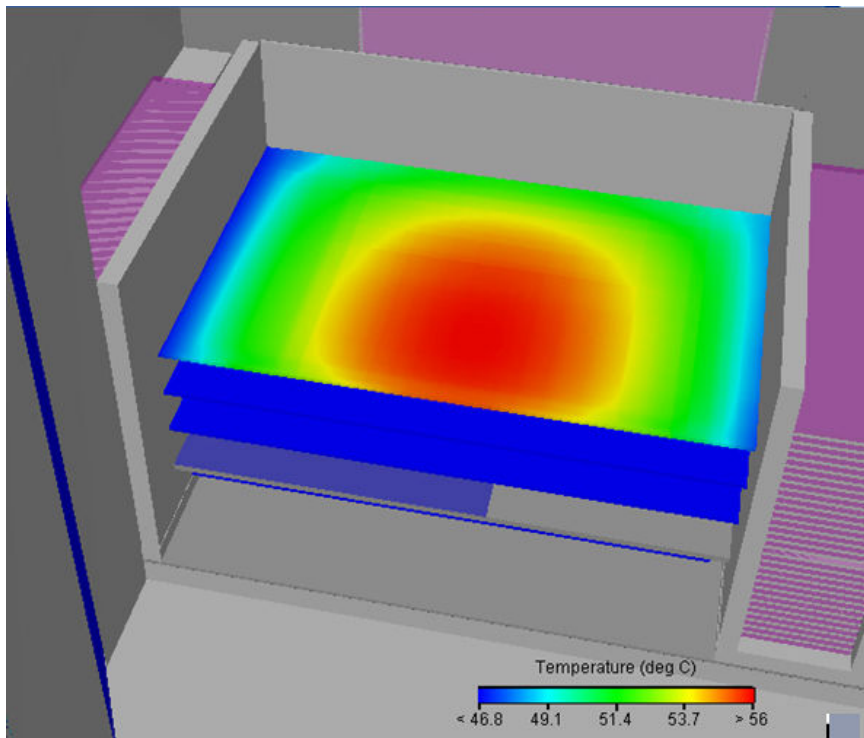


Fig. 9-9 Predicted temperature profile of HRDL board for Case 1



CARLO GAVAZZI SPACE SpA

ACOP

THERMAL ANALYSIS AND DESIGN REPORT

Doc N°:

ACP-RP-CGS-006

Issue:

2

Date:

Oct. 2005

Page

33

of

44

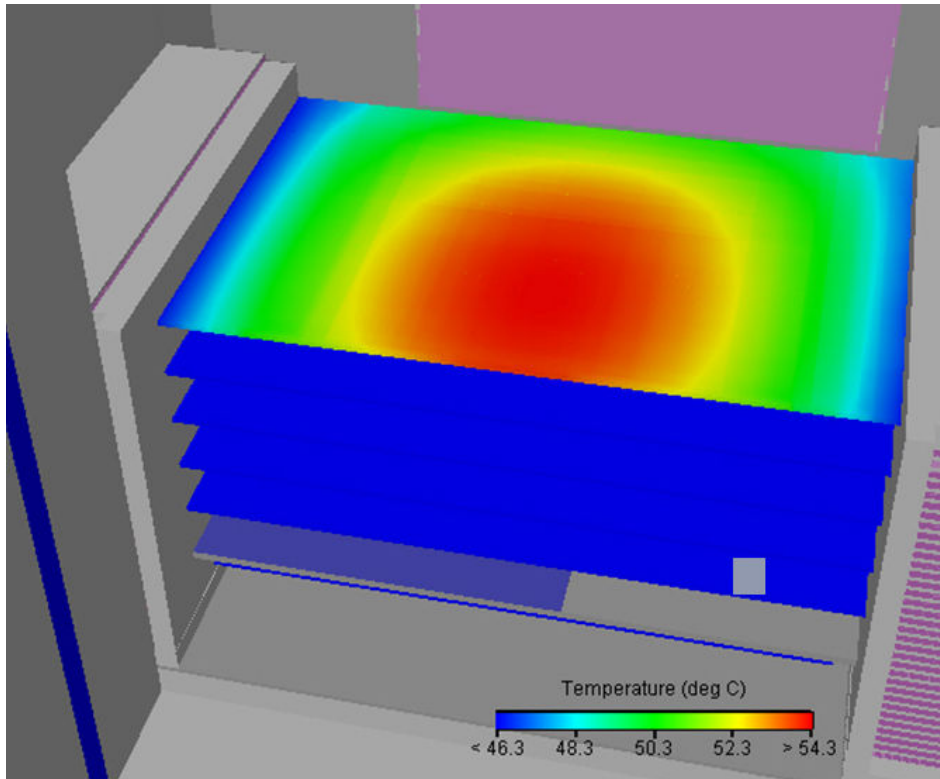


Fig. 9-10 Predicted temperature profile of spared board for Case 1

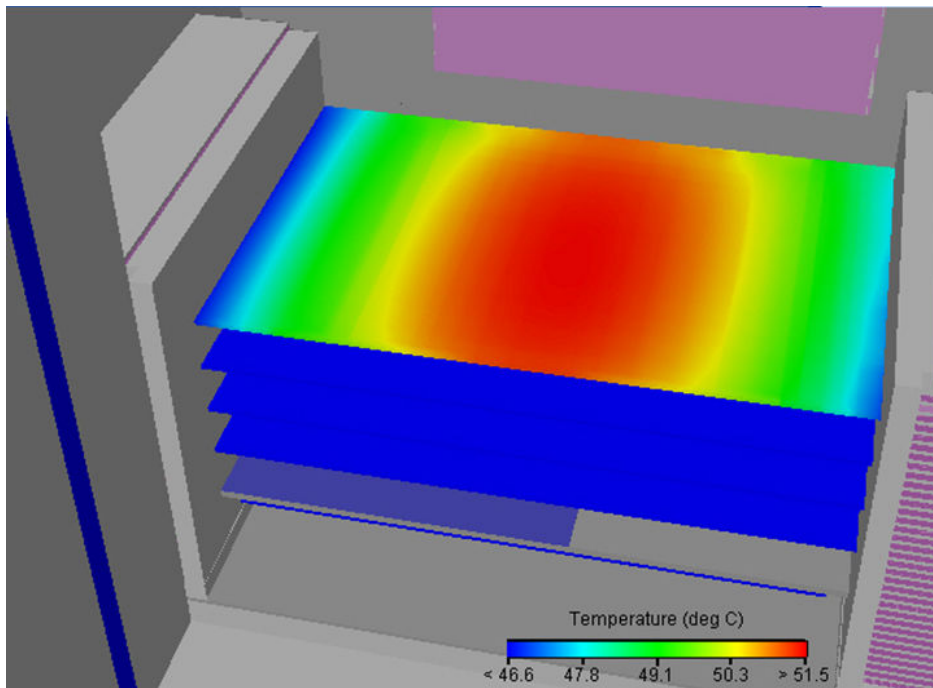


Fig. 9-11 Predicted temperature profile of SATA plus Ethernet board for Case 1.

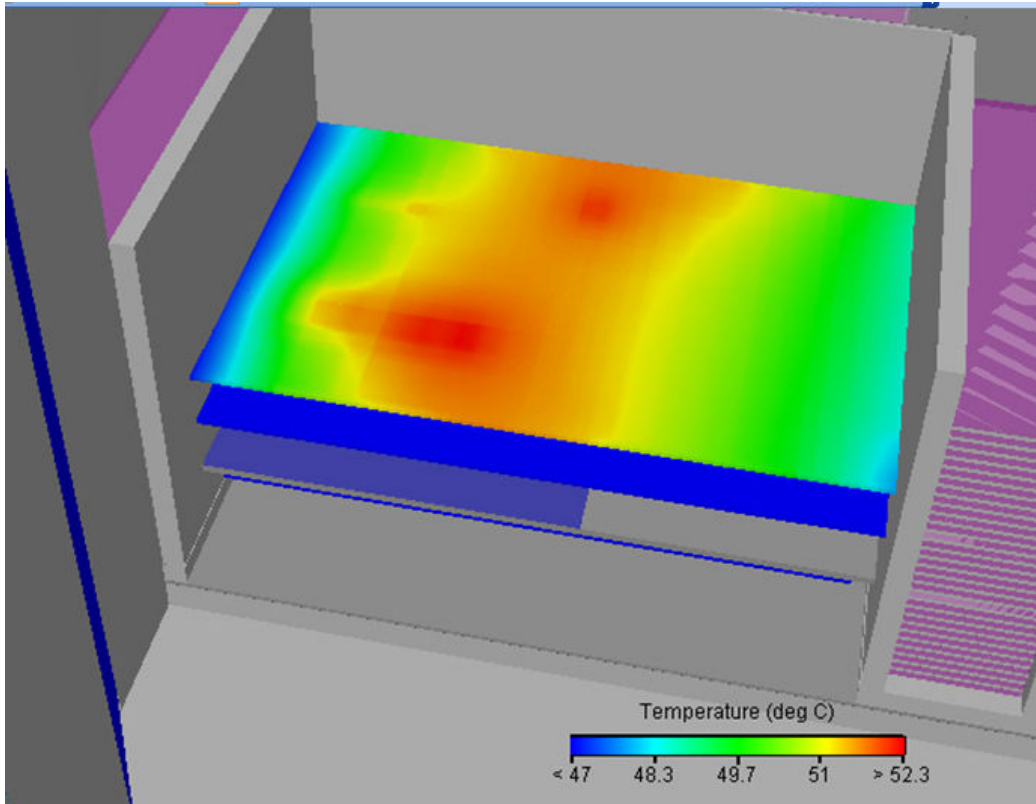


Fig. 9-12 Predicted temperature profile of USB plus Video board for Case 1

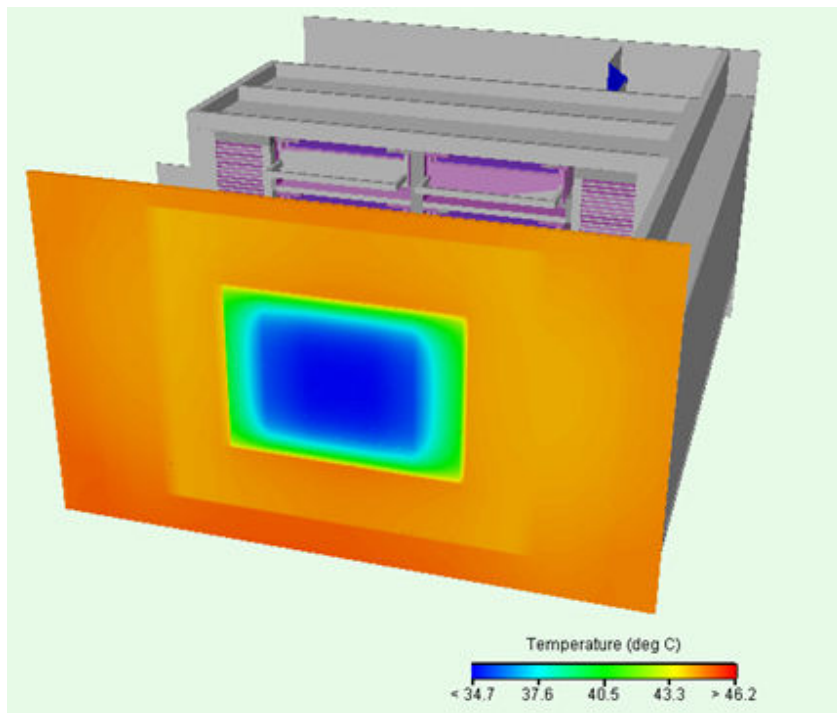


Fig. 9-13 Predicted temperature profile of the front panel for Case 1

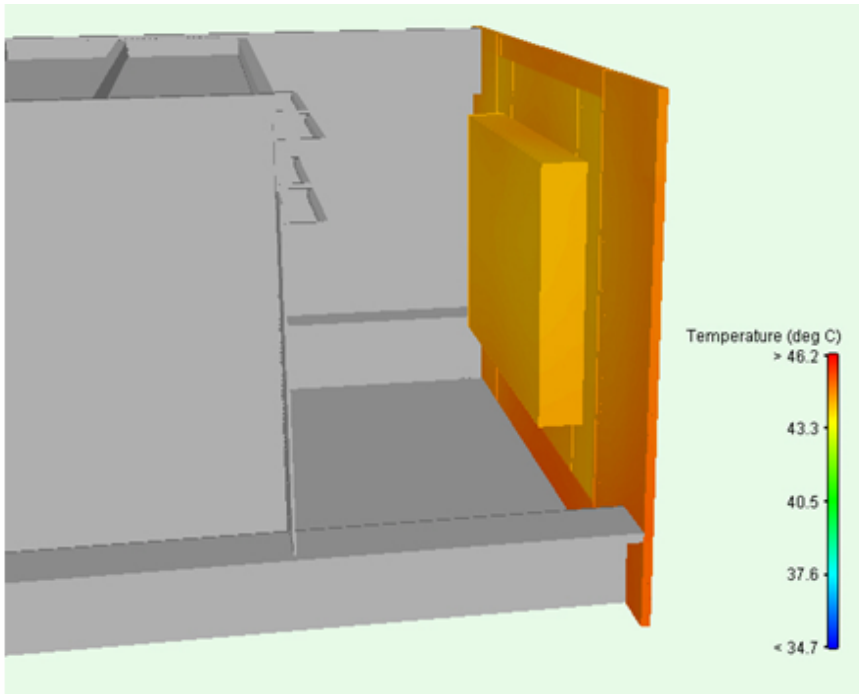


Fig. 9-14 Predicted temperature profile of the front panel back for Case 1

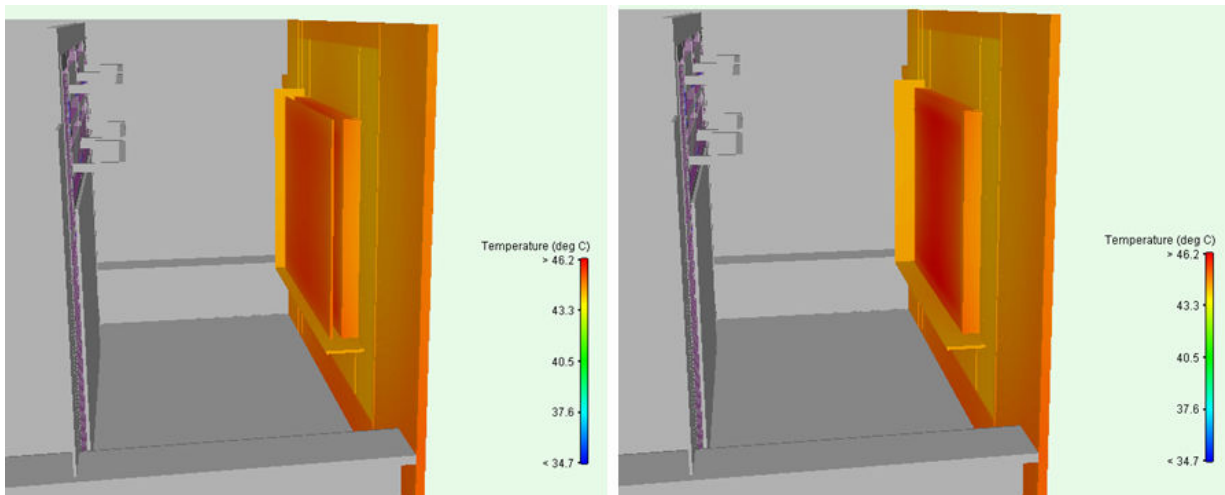


Fig. 9-15 Predicted temperature for LCD assembly details in Case 1

9.2 CASE 2: INLET FAN ON AND OUTLET FAN OFF

For Case 2, the power dissipation of the inlet fan will influence air temperature and therefore ACOP temperatures.

The cooling air velocity field at the X-Z plane along the centre of the channel is shown in Fig. 9-16.

As the cooling air enters ACOP, the air velocity profile does not change significantly till ahead of the inlet channels and the HDD's gap, where the air velocity becomes more uniform.

As described for Case 1, the flow impedance of the inlet fin channels is much larger than that of the HDD's gap while with the same air velocity. Thus, a large portion of the coming air enters into the HDD's gap and the less rest air goes through the fin channels. The predicted maximum velocity is 1.41 m/sec in the outlet fin channels.

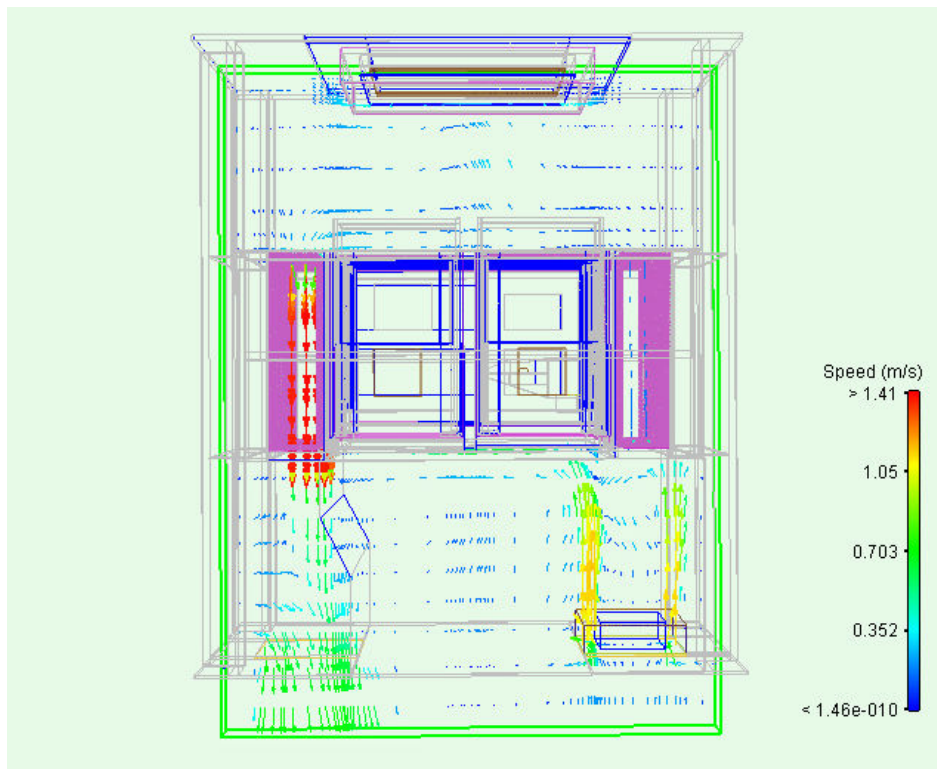


Fig. 9-16 Predicted velocity field of the cooling air in ACOP at the cross section of the fin channel centre along X-Z plane for Case 2

The predicted results indicate that the maximum pressure head of the fan for the intake air into ACOP is around 7.5Pa. Similar to Case 1, most of the pressure loss occurs in the outlet fin channels, resulted from the large air velocity and a high friction coefficient. A small part of the pressure head compensate the loss of the flow in the inlet fin channels or in the HDD's gap, the off outlet fan with the filters, and the interfaces between the chambers and the fin channels.



CARLO GAVAZZI SPACE SpA

ACOP

THERMAL ANALYSIS AND DESIGN REPORT

Doc N°:

ACP-RP-CGS-006

Issue:

2

Date:

Oct. 2005

Page

37

of

44

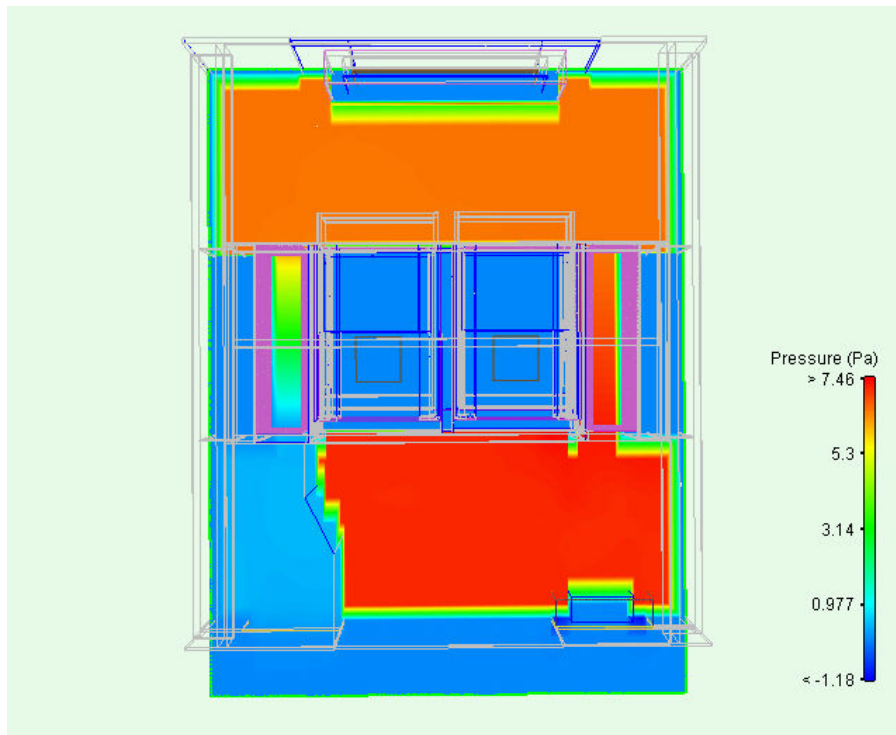


Fig. 9-17 Predicted pressure distribution for case 2

Fig. 9-18 and *Fig. 9-19* show the temperature of ACOP of the fin channel along X-Z plane and of the centre cross section along X-Y plane with a fan to exhaust air out.

The inlet fin temperature is predicted to be around 46°C at most of the regions due to a small flow rate passing through the inlet fin channels, resulting into a rapid increase temperature of the cooling air in the inlet fin channels.

While the temperature of air in the HDDs gap does not increase as significantly as in the inlet fin channels

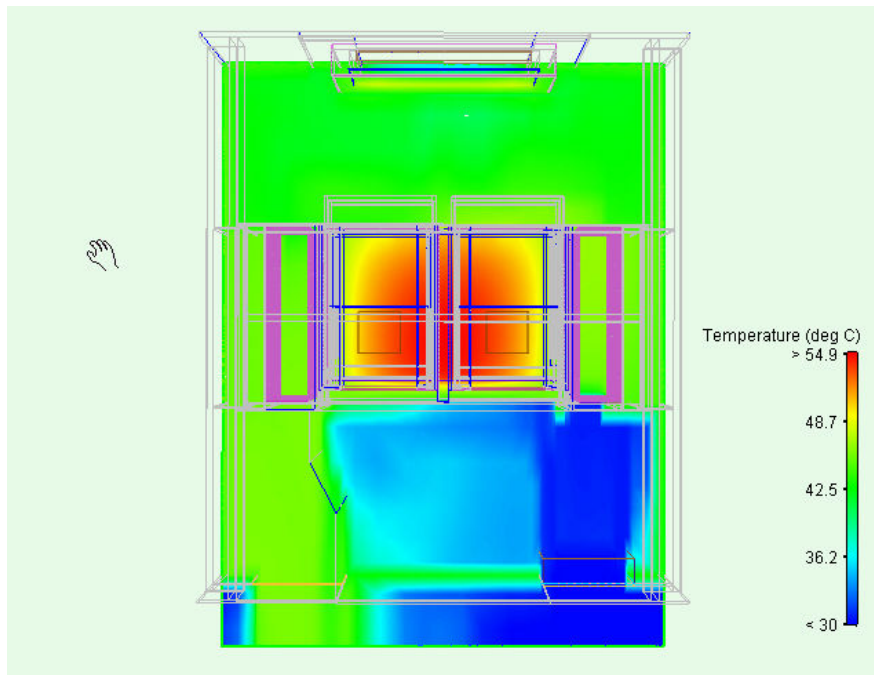


Fig. 9-18 Predicted temperature profile of ACOP of the fin channel along X-Z plane for Case 2

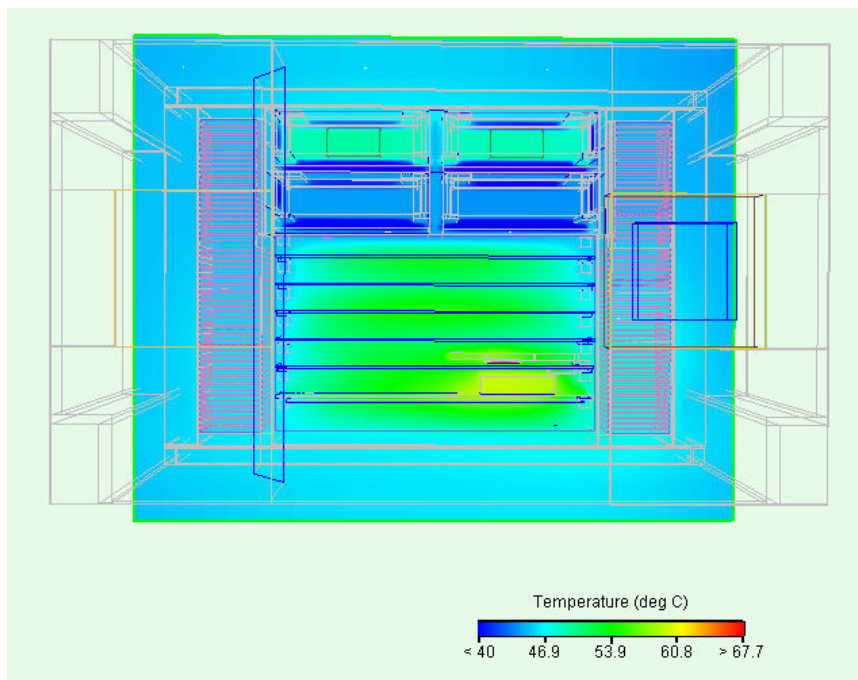


Fig. 9-19 Predicted temperature profile of ACOP of the centre cross section along X-Y plane for Case 2



CARLO GAVAZZI SPACE SpA

ACOP

THERMAL ANALYSIS AND DESIGN REPORT

Doc N°:

ACP-RP-CGS-006

Issue:

2

Date:

Oct. 2005

Page

39

of

44

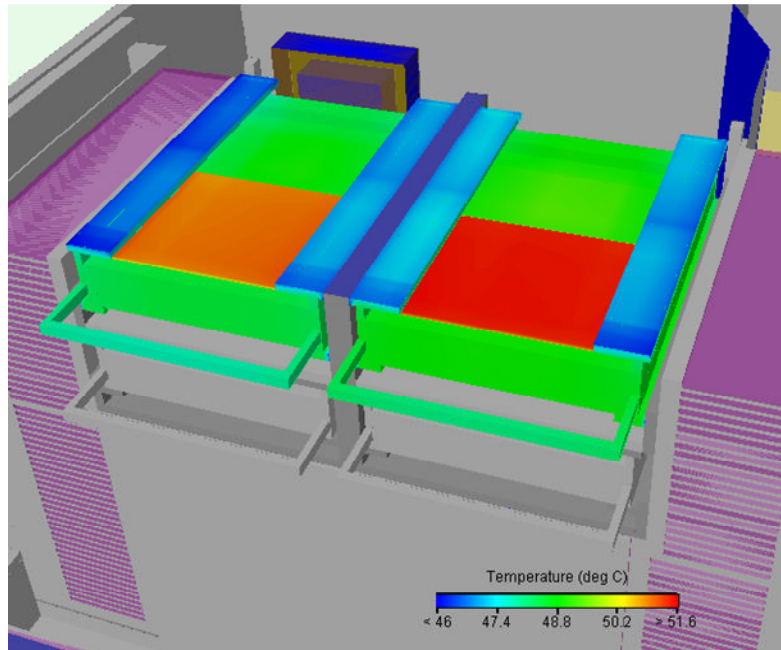


Fig. 9-20 Predicted temperature of working HDD's for Case 2

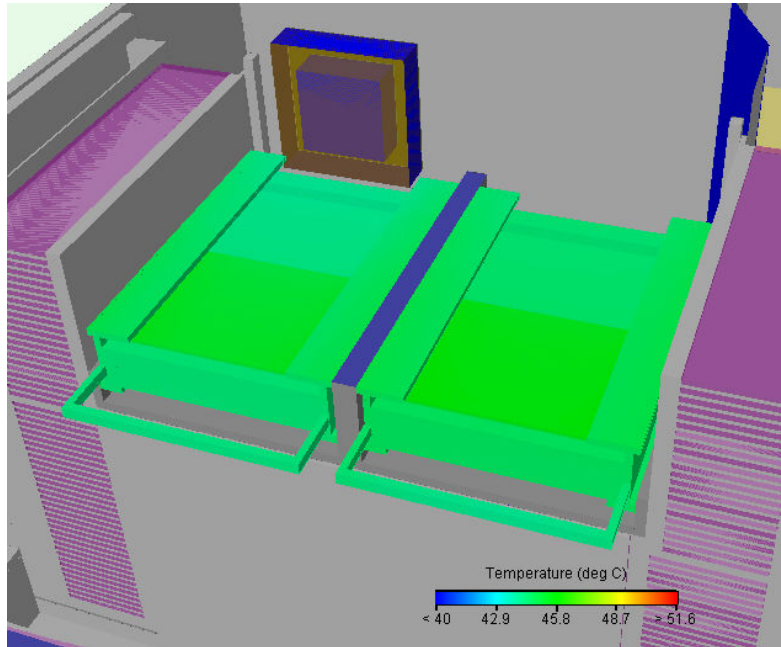


Fig. 9-21 Predicted temperature o HDD's in stand by for Case 2

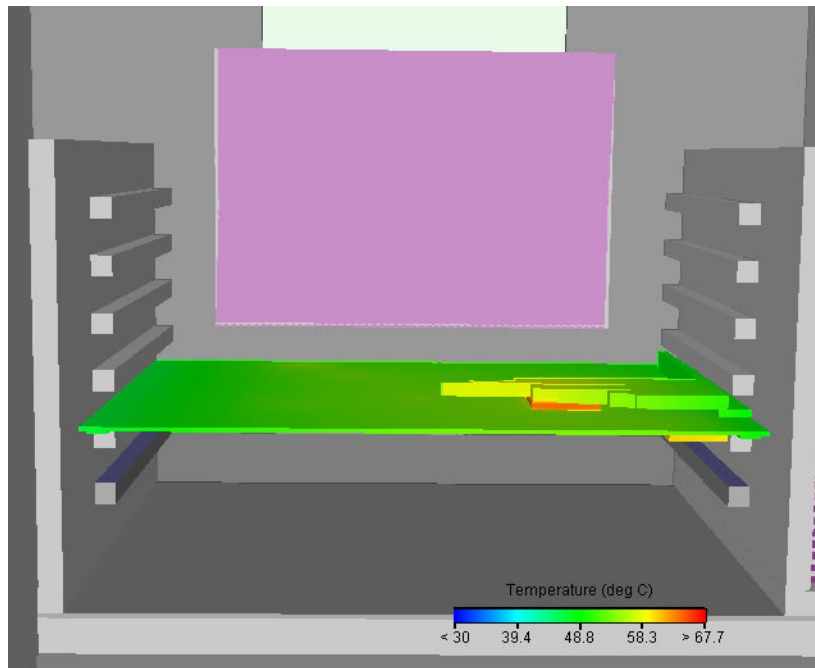


Fig. 9-22 Predicted SBC board temperature at the component side for Case 2

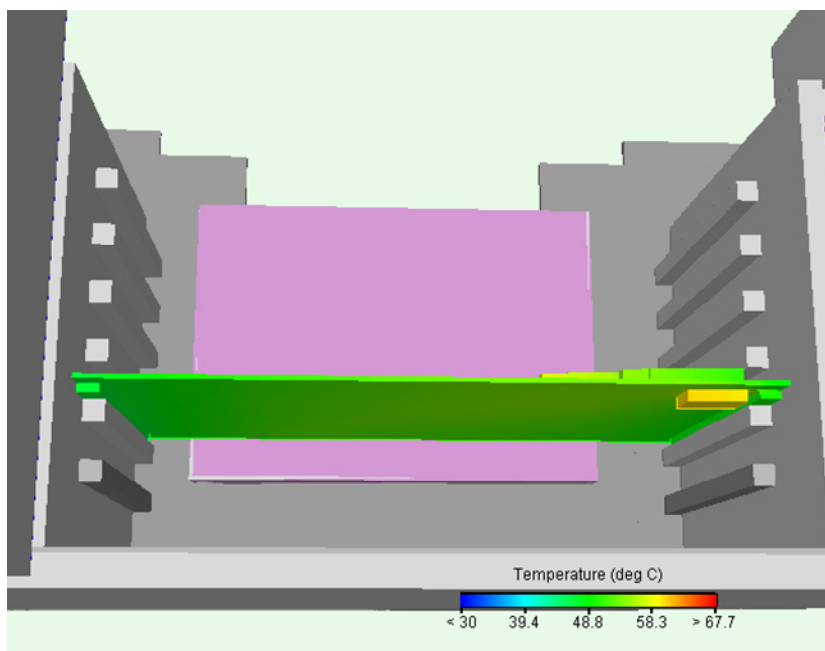


Fig. 9-23 Predicted SBC board temperature at the solder side for Case 2



CARLO GAVAZZI SPACE SpA

ACOP

THERMAL ANALYSIS AND DESIGN REPORT

Doc N°: **ACP-RP-CGS-006**

Issue: **2** Date: **Oct. 2005**

Page **41** of **44**

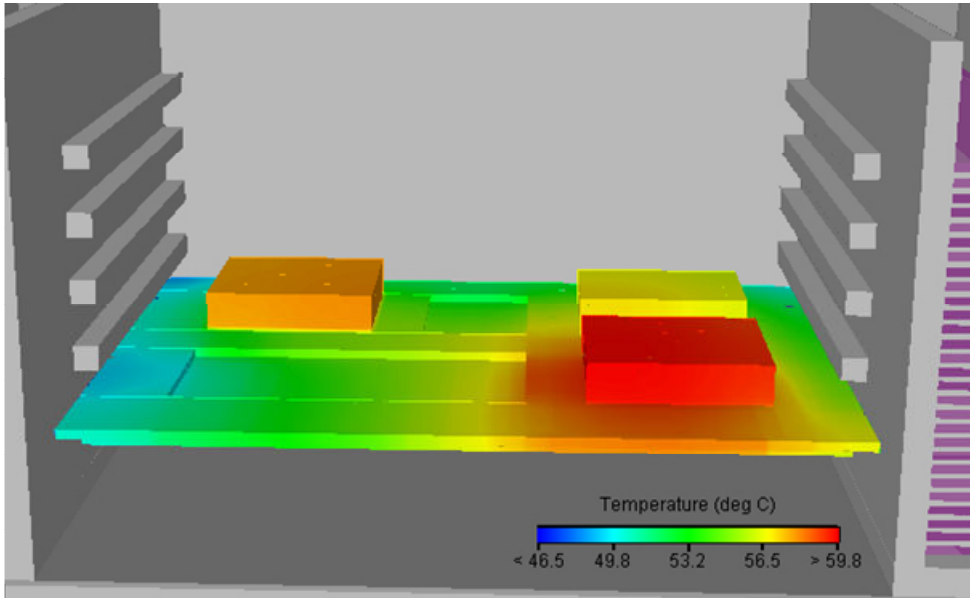


Fig. 9-24 Predicted temperature profile of power distribution board for Case 2.

9.3 SUMMARY OF THE RESULTS IN CASE 1 AND 2

	Temperature in case 1 (°C)	Temperature in case 2 (°C)
Chassis (@outlet of outlet fins)	47.4	46.8
working HDD	49.4	49.0
stand by HDD	44.9	44.4
control board of working HDD	51.7	51.3
control board of stand by HDD	45.1	44.6
SBC Die	68.5	67.7
SBC Regulator	60.7	60.0
SBC Microprocessor	67.9	67.2
PS Converter max.	57.7	57.0
HRDL max.	54.9	54.3
Spare max.	54.0	53.4
SATA+Ether max.	51.5	50.9
USB+Videomax.	51.7	51.2
PS card edge	48.9	48.3
HRDL card edge	48.5	47.8
Spare card edge	47.4	46.8
SATA+Ether card edge	47.8	47.1
USB+Video card edge	48.7	48.0
LCD VI board	45.5	45.2
LCD	46.0	45.6
Lexan (center)	34.9	34.8
average front panel (including Lexan)	43.3	43.0
air exhaust	46.2	45.7

Tab. 9-1 Summary of the results for case 1 and 2

9.4 CASE 3: BOTH FANS FAILED

In order to understand the temperature rising of ACOP when both fans are failed, the thermal analysis of ACOP in transient mode with fans off after the steady state operation is also carried out and denoted as Case 3.

The heat exchange path between ACOP and the environment is only through the front panel to the ISS cabin. The computation period is taken four hours after fans failed. The time step of the computation is set to be 5 seconds.

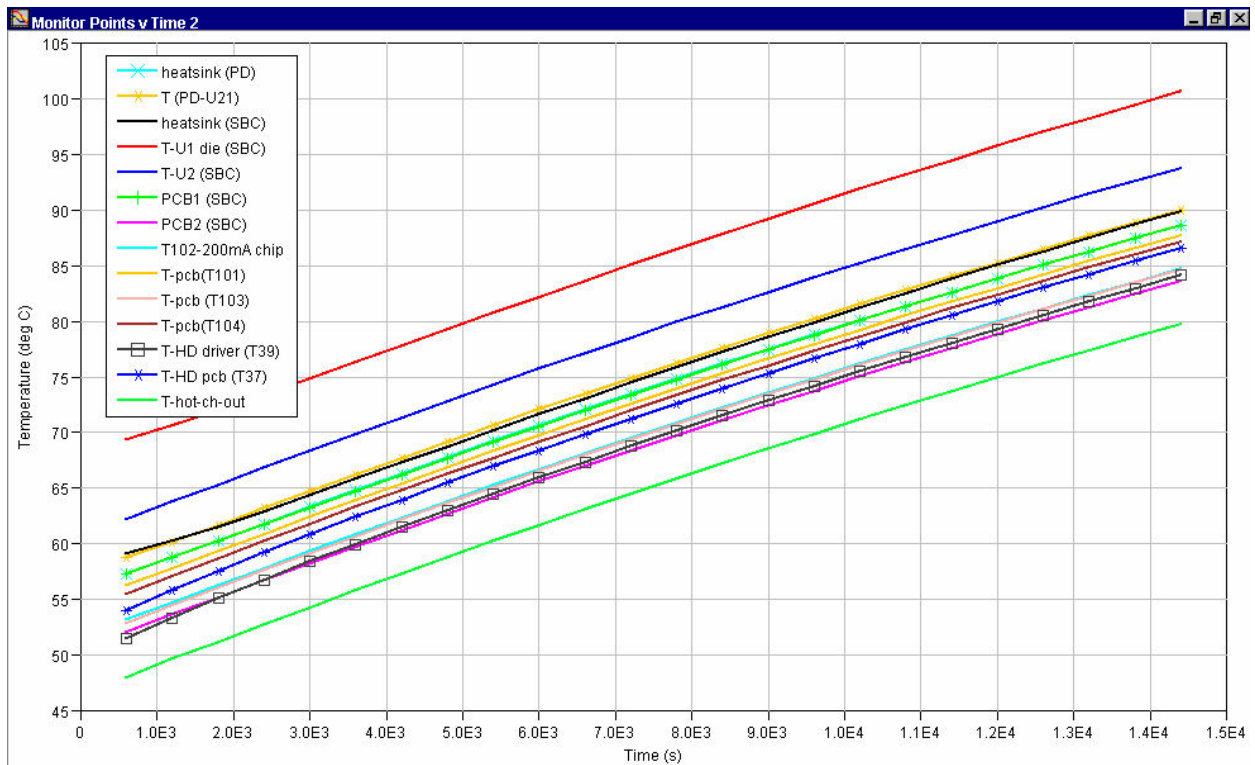


Fig. 9-25 Predicted temperature histories of main components or parts after two fans failed

 CARLO GAVAZZI CARLO GAVAZZI SPACE SpA	<h1>ACOP</h1>	Doc N°: ACP-RP-CGS-006
	THERMAL ANALYSIS AND DESIGN REPORT	Issue: 2 Date: Oct. 2005 Page 43 of 44

9.5 HEAT REJECTION TO THE ENVIRONMENT AND ADJACENT LOCKERS

Under the model computation, ACOP is assumed insulated from the adjacent Lockers and the Rack. This is a design assumption adopted to optimize ACOP thermal design, as discussed in section 6.1.

However, at actual condition, the adjacent lockers and rack surfaces will interface with ACOP. In this paragraph a calculation of the heat exchange rate between ACOP and the adjacent Lockers, the Rack, and the ISS cabin.

The emissivity is 1.0 except for the front panel, of which value is taken as 0.82. The convection is considered only for the front panel with the ISS cabin, as indicated in the IDD.

The temperature considered for the adjacent surfaces is the maximum temperature defined in the IDD. The heat exchange results for the minimum temperature of the adjacent surfaces is not performed since ACOP temperature and adjacent items temperatures all depend on the temperature of the cooling system. It would be therefore not representative to have ACOP at ~45°C and adjacent surfaces at 18°C.

	ACOP sides average Temperature	Interface Equipment	Hot I/F Temperature	Heat exchange
Front plate	44°C	ISS cabin	30°C	11.1W
Inlet side plate	43°C	Rack	40°C	3.1W
Outlet side plate	45°C	Rack	40°C	8.6W
Bottom plate	47°C	Locker	50°C	-5.5W
Top plate	45°C	Locker	50°C	-5.4W

Tab. 9-2 Heat exchange rate between ACOP and the surroundings at two extreme conditions

 CARLO GAVAZZI SPACE SpA	<h1>ACOP</h1>	<i>Doc N°:</i> ACP-RP-CGS-006
	THERMAL ANALYSIS AND DESIGN REPORT	<i>Issue:</i> 2 <i>Date:</i> Oct. 2005 <i>Page</i> 44 <i>of</i> 44

10 CONCLUSIONS

Fans have been introduced at the inlet and outlet of ACOP, providing 12cfm airflow rate. One fan will be working at a time. The inlet fan working only and the outlet fan working only will have the same air flow rate of 12cfm. The temperature results between these two cases are therefore very similar and the temperatures of all critical components are below the allowable temperatures.

The requirement on crew touch temperature on the front panel (49°C) is met.

The front panel average temperature is predicted to be 44°C and the requirement on average temperature of the front panel is however not met. The reason of this requirement is however not completely understood. Major design modifications should be avoided due to their consequences on the mass budget and in particular on CoG position and structural analysis results.

The average temperature requirement could be discussed with NASA to investigate if it is possible to relax it, since no continuous touch is foreseen on ACOP surface when operative (only push buttons are touched).

The outlet temperature of the cooling air is calculated to be around 47°C if the minimum flow rate is supplied, which is still less than the requirements of the exhaust temperature 49°C in AD1.

If the fans are failed, the commercial HDDs can work for around two and a half hours if the allowable HDD board temperature is set to be 70°C. However, the main components, i.e. the SBC microprocessor, and the DC-DC converters can survive for more than four hours, resulting from the good thermal management by using heat sinks for these components.